

Yuwei Kan and Qiang Zhang

## Abstract

Hydrogen activation is a very important industrial process for hydrogenation reactions and ammonia production. The hydrogen splitting and hydride transfer process can be classified as homolytic and heterolytic cleavage of molecular hydrogen on mono- and multinuclear transition metal centers. Hydrogenase enzymes have inspired researchers in the field of organometallic chemistry to develop small molecule structural models of active sites and thus to mimic the biological system to activate molecular hydrogen. Multinuclear cluster complexes, including those containing heavy main group metals, can bind hydrogen molecule under mild conditions in a reversible fashion. This chapter aims at providing introductory review to cover various types of transition metal complexes that can split molecular hydrogen. The interaction between hydrogen molecule and metal centers, which determines the distance between two hydrogen atoms, will affect hydrogen splitting. The mechanism of such interactions will be discussed in details. Hydrogenation reactions catalyzed by transition metal complexes or heterogeneous nanocatalysts derived from metal cluster complexes will also be introduced.

**Author Contribution:** The chapter context was mainly compiled by Dr. Y. Kan under the supervision of Dr. Q. Zhang. The introduction part, chemical expression, and the revision of other subsections were examined and corrected by Dr. J. Liu and Dr. S. Bashir.

Y. Kan

Department of Chemistry, Texas A&M University, College Station, TX, USA

Department of Chemistry, Washington State University, Pullman, WA, USA

e-mail: [yuwei.kan@chem.tamu.edu](mailto:yuwei.kan@chem.tamu.edu)

Q. Zhang (✉)

Department of Chemistry, Washington State University, Pullman, WA, USA

e-mail: [q.zhang@wsu.edu](mailto:q.zhang@wsu.edu)

### Abbreviations

BAr <sup>F</sup>	[B{C <sub>6</sub> H <sub>3</sub> (CF <sub>3</sub> ) <sub>2</sub> } <sub>4</sub>
Bn	Benzyl
bq	7,8-Benzoquinolato
CDA	Cyclododecane
CDE	Cyclododecene
CDT	Cyclododecatriene
COD	1,5-Cyclooctadiene
Cp	η <sup>5</sup> -Cyclopentadienyl
Cy	Cyclohexyl
DFT	Density functional theory
depe	1,2-bis(diethylphosphino)ethane
dppe	1,2-bis(diphenylphosphino)ethane
EAC	Ethyl (Z)-1-acetamidocinnamate
EPR	Electron paramagnetic resonance
EXAFS	Extended X-ray absorption fine structure
Fc	Ferrocene
NMR	Nuclear magnetic resonance
PCy <sub>3</sub>	Tricyclohexylphosphine ligand
P <sup>i</sup> Pr <sup>3</sup>	Triisopropylphosphine ligand
PR <sub>2</sub>	Phosphido ligand
PR <sub>3</sub>	Phosphine ligand
Py	Pyridine
ROP	Ring opening polymerization
TOF	Turnover Frequency
Tp	Trispyrazolylborate

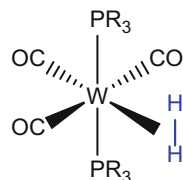
### Contents

2.1	Introduction and Background .....	44
2.2	Molecular Complexes for Hydrogen Activation .....	49
2.2.1	Hydrogen Activation by Mononuclear Transition Metal Complexes .....	49
2.2.2	Heterometallic Cluster Complexes for Hydrogen Activation .....	58
2.3	Supported Nanoclusters for Hydrogenation Reactions .....	67
2.3.1	Transition Metal Cluster Complexes as Precursors for Heterogeneous Hydrogenation .....	69
2.3.2	Heavy Main Group Metal Modified Transition Metal Clusters as Supported Catalysts for Hydrogenation .....	74
2.4	Summary .....	77
	References .....	78

## 2.1 Introduction and Background

Hydrogen gas (H<sub>2</sub>) as an energy carrier has historically played an important role, for example production of synthetic methanol through steam reforming by BASF in Leuna, Germany, in 1923, and plays a vital role in a variety of industrial processes,

**Scheme 2.1**  $W(CO)_3(PR_3)_2(H_2)$  discovered by Kubas in 1984



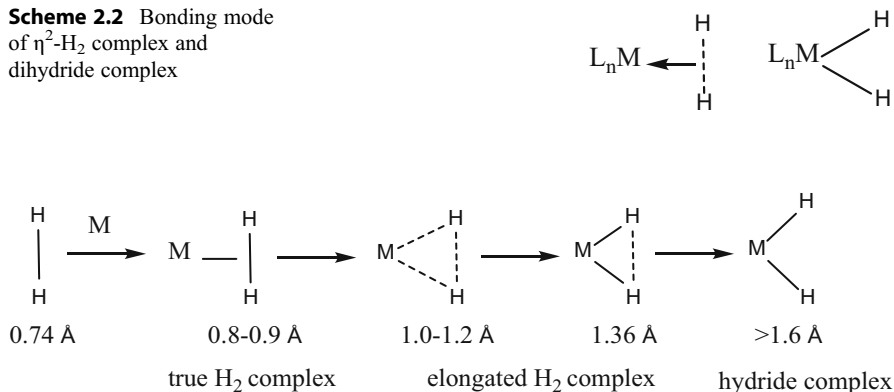
such as hydrogenation reactions, the production of ammonia ( $NH_3$ ) from  $H_2$  and nitrogen ( $N_2$ ) that greatly supports the world's agriculture; and the processing of petrochemical in which crude oil is treated with  $H_2$ . Hydrogen is also considered as valuable future fuel which is environmental friendly. It attracts considerable attention to scientists all over the world to develop new plans for hydrogen storage and production.  $H_2$  molecule has a very low chemical reactivity due to the very strong, nonpolar covalent bond, which holds together the two hydrogen atoms. In order to improve the efficient utilization of  $H_2$ , transition metal catalysts are often required to facilitate H–H bond splitting process.

The activation of molecular hydrogen by transition metal complexes is of great importance in organometallic chemistry and is an essential step in understanding catalytic hydrogenation processes [1, 2]. The interaction of  $H_2$  with transition metal complexes results in the perturbation of H–H bond which leads to the formation of a mono- or dihydride complex. Since the discovery of the first transition metal hydride complex,  $H_2Fe(CO)_4$ , in 1931 by Hieber, along with the development of various characterization techniques, such as single crystal X-ray diffraction analyses and neutron scattering, a vast number of transition metal hydride complexes were synthesized, characterized [3, 4], and can be used in homogeneous hydrogenation system [5, 6]. Thousands of papers and lots of review articles were published on this subject [7, 8]. However, the hydrogen activation mechanism was not established until 1980s. Particularly, the discovery of the first stable dihydrogen complex which contains intact molecular  $H_2$  in transition metal complex,  $W(CO)_3(PR_3)_2(H_2)$  (where  $PR_3$  is a phosphine ligand), by Kubas in 1984 significantly propelled the development of the field of hydrogen activation (as shown in Scheme 2.1) [9].

There are numerous review articles and book chapters published in recent years provide important summaries regarding the theories and properties of transition metal dihydrogen complexes [10–14].  $H_2$  interacts with metal center in a side-on ( $\eta^2$ ) mode (as shown in Scheme 2.2) by donating its two  $\sigma$  electrons to a vacant metal  $d$  orbital, forming a nonclassical 3-center 2-electron ( $3c-2e$ ) bond, which elongates the H–H bond. The stability of  $\eta^2-H_2$  complex depends on the strength of electron back-donation from a filled  $d$  orbital of the metal center to the  $\sigma^*$  orbital of  $H_2$ . Therefore, in some cases the strong back-donation causes the splitting of dihydrogen to dihydride complexes with elongated H–H bond distance (as shown in Scheme 2.3) [11].

As mentioned in the beginning of the introduction, hydrogenation reaction is one of the most important industrial processes. Most hydrogenation reactions [ $RCH=CH_2 + H_2 \rightarrow RCH_2CH_3$  ( $R = \text{alkyl, aryl}$ )] use hydrogen gas to reduce or saturate organic compounds. Transition metal complexes are commonly involved as

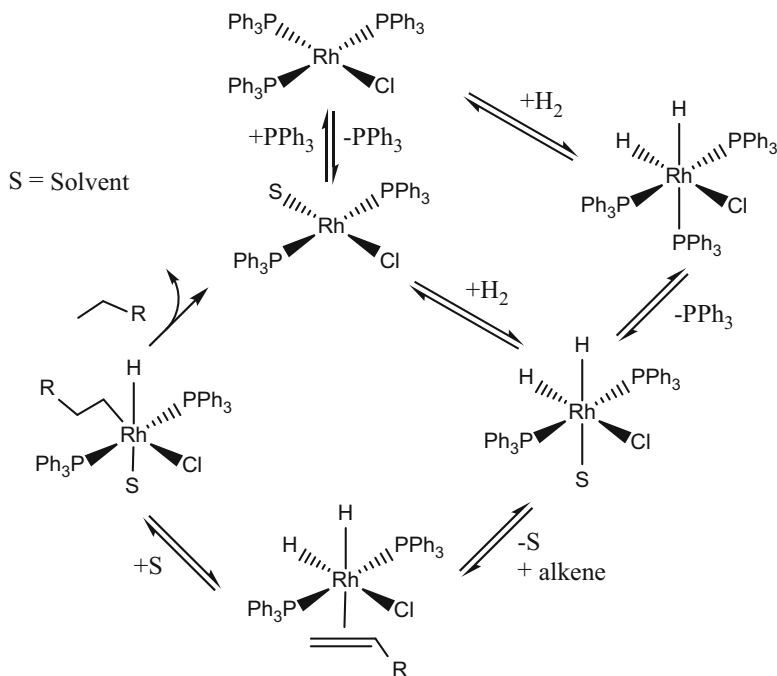
**Scheme 2.2** Bonding mode of  $\eta^2$ -H<sub>2</sub> complex and dihydride complex



**Scheme 2.3** H–H bond distances from crystallography and NMR

either homogeneous [e.g., C<sub>10</sub>H<sub>14</sub>O + 1 atm H<sub>2</sub> + RhCl(PPh<sub>3</sub>)<sub>3</sub> where PPh<sub>3</sub> is triphenylphosphine → C<sub>10</sub>H<sub>16</sub>O] or heterogeneous [e.g., C<sub>8</sub>H<sub>6</sub> + 1 atm H<sub>2</sub> + [5% Pd-CaCO<sub>3</sub> + Pb(OCOCH<sub>3</sub>)<sub>2</sub> + C<sub>9</sub>H<sub>7</sub>N] → C<sub>8</sub>H<sub>8</sub>] catalysts to facilitate this process and improve the selectivity of desired hydrogenation product [15–17]. Transition metal complexes, such as Rh, Ir complexes, are long known to homogeneously catalyze hydrogenation reaction by promoting molecular hydrogen activation [18, 19]. Transition metal hydrides are normally involved as intermediates in the catalytic cycle. Wilkinson's catalyst, RhCl(PPh<sub>3</sub>)<sub>3</sub>, was discovered in 1965 as the first highly active homogeneous hydrogenation catalyst that is used under mild conditions [20]. It is well known to catalyze hydrogenation of alkene (as shown in Scheme 2.4) to alkane. In this catalytic cycle, one bulky triphenylphosphine ligand on RhCl(PPh<sub>3</sub>)<sub>3</sub> is readily lost to form highly unsaturated 14-electron rhodium complex RhCl(PPh<sub>3</sub>)<sub>2</sub> due to steric effect, followed by rapid oxidative addition of hydrogen molecule to produce 16-electron dihydride complex RhClH<sub>2</sub>(PPh<sub>3</sub>)<sub>2</sub>. The next step, alkene is coordinated to rhodium via  $\pi$  donation and followed by intramolecular hydride transfer to yield alkyl hydride intermediate, RhH(alkyl)Cl(PPh<sub>3</sub>)<sub>2</sub>, which finally results in alkane product and regenerates RhCl(PPh<sub>3</sub>)<sub>2</sub> through reductive elimination.

Other than Wilkinson's catalyst, there are two other famous cationic homogeneous hydrogenation catalysts: one is rhodium based Schrock-Osborn catalyst [21], [Rh(COD)(PPh<sub>3</sub>)<sub>2</sub>]<sup>+</sup>, (where COD = 1,5-cyclooctadiene) and the other one is iridium based Crabtree's catalyst [Ir(COD)(PCy<sub>3</sub>)(Py)]<sup>+</sup> (Py = pyridine, Cy = cyclohexyl) [22]. They are more active and effective for hydrogenation reaction than Wilkinson's catalyst. The cationic metal center is more electrophilic than neutral metal center and thus fosters the coordination of alkene, which is the essential reaction rate determination step. These catalysts also exhibit high activity in the hydrogenation of hindered alkene. Notably, Crabtree's catalyst even catalyze the hydrogenation of tetra-substituted olefin compounds, while Wilkinson's and Schrock-Osborn catalysts do not. The hydrogenation rate of various substituted olefins with different Ir and Rh catalysts is shown in Table 2.1 [22].



**Scheme 2.4** Catalytic hydrogenation of alkene by Wilkinson's catalyst

**Table 2.1** Rates<sup>a</sup> of hydrogenation of substituted olefins with different catalysts

Catalyst	Temp °C	Solvent	Substrate			
			1-hexene	Cyclohexene	1-Methylcyclohexene	2,3-Dimethylbut-2-ene Me <sub>2</sub> C = CMe <sub>2</sub>
[Ir(COD)(PCy <sub>3</sub> )(py)] <sup>+</sup>	0	CH <sub>2</sub> Cl <sub>2</sub>	6400	4500	3800	4000
[Ir(COD)(PMePh <sub>2</sub> ) <sub>2</sub> ] <sup>+</sup>	0	CH <sub>2</sub> Cl <sub>2</sub>	5100	3800	1900	50
	0	acetone	~10	0	0	0
[Rh(COD)(PPh <sub>3</sub> ) <sub>2</sub> ] <sup>+</sup>	25	CH <sub>2</sub> Cl <sub>2</sub>	4000	10	–	0
HRuCl(PPh <sub>3</sub> ) <sub>3</sub>	25	C <sub>6</sub> H <sub>6</sub>	9000	7	–	0
RhCl(PPh <sub>3</sub> ) <sub>3</sub>	25	C <sub>6</sub> H <sub>6</sub> / EtOH	650	700	13	0
	0	C <sub>6</sub> H <sub>6</sub> / EtOH	60	70	–	0

<sup>a</sup>In mol of substrate reduced (mol of catalyst)<sup>-1</sup> h<sup>-1</sup>

Heterogeneous catalytic hydrogenation is more widely used in industry. Heterogeneous catalysts are present in different phase from reactants, which are often recovered and recycled for cost savings. Heterogeneous hydrogenation reaction occurs on the interfaces of catalysts and reactants. In other words, adsorption of reactant,

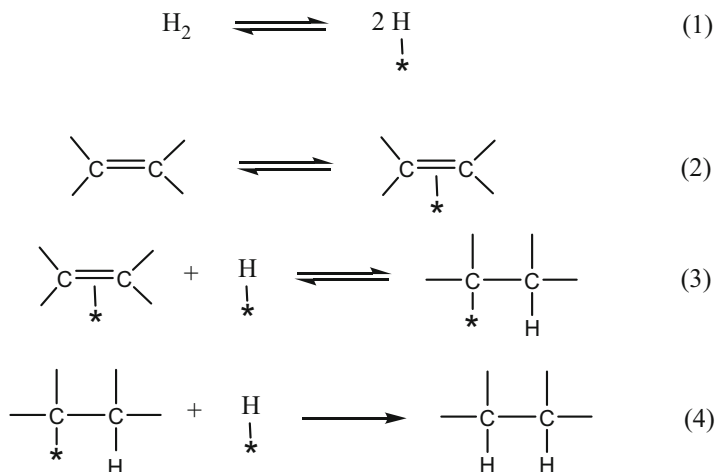


**Fig. 2.1** The alkene hydrogenation mechanism proposed by Horiuti-Polanyi.

hydrogenation chemical reaction, and desorption of product must take place on the surface of catalysts [23]. The bond of reactant should be weakened or broken with the formation of reactive intermediates. An example is provided to illustrate the hydrogenation of alkene using a heterogeneous catalyst (Fig. 2.1). Hydrogen is adsorbed to the catalyst surface, followed by the cleavage of H–H  $\sigma$  bond to form more reactive M–H bonds. C=C  $\pi$  bond of alkene is weakened by adsorption to catalyst surface and then reacts with the activated hydrogen in a stepwise process to eventually yield alkane. This mechanism for alkene hydrogenation was proposed by Horiuti and Polanyi in 1934 [24].

Heterogeneous catalysts are normally transition metal, metal alloy, or metal oxides. The catalyst can be deposited on support with high surface area to foster hydrogen diffusion and promote interaction between catalysts and reactants. Heterogeneous catalysis seems to be far away from the area of organometallic chemistry at the first sight; however, surface organometallic species are often involved during the process of hydrogenation. Moreover, transition metal cluster complexes have been used as precursors to generate heterogeneous catalyst. Cluster chemistry can also serve as effective structural model to study the behavior of small molecules on metal surfaces in chemisorbed processes, which is known as the cluster-surface analogy [25, 26]. Further discussion will be provided in Sect. 2.2.

Hydrogenase enzymes are also one important class of compounds that are known for the activation of hydrogen in biological system. They are active redox enzymes that catalyze reversible oxidation of hydrogen to protons (Eq. 2.1). There are mainly three types of active sites in hydrogenase, [Fe]-only hydrogenase, dinuclear [FeFe] hydrogenases, and [NiFe] hydrogenases. A reversible hydrogen oxidation reaction is shown in Eq. 2.1.



X-ray crystallography and spectroscopic analyses revealed that the active sites at hydrogenase enzymes are organometallic complexes of Fe or Ni. While precious metal catalysts are majorly used in industry, nature has its unique way to reversibly activate hydrogen by using first row transition metals. Synthetic organometallic chemists are inspired by nature to pursue the synthesis of first row transition metal complexes by mimicking the function of hydrogenase in order to obtain efficient and inexpensive catalysts for hydrogen oxidation and production. This chemistry has been developed explosively since 2000 when the comprehensive review article came out by Marcetta Y. Darensbourg [27]. This book chapter (Sect. 2.2.2) will mainly focus on the introduction of structure model of the active site on hydrogenase, and a few examples of hydrogen activation process by the synthetic organometallic complexes will also be provided.

## 2.2 Molecular Complexes for Hydrogen Activation

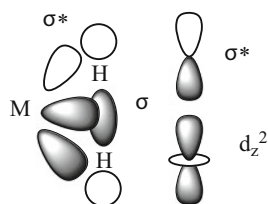
### 2.2.1 Hydrogen Activation by Mononuclear Transition Metal Complexes

The majority well-studied organometallic compounds for hydrogen activation are mononuclear transition metal complexes. Metal dihydrogen complexes are stabilized by electronic synergistic effect of  $\sigma$  electron donation from dihydrogen and electron backdonation from  $d$  orbital of metal center to the  $\sigma^*$  orbital of dihydrogen (Scheme 2.5). There are two different ways to split H–H bond by transition metal complexes: homolytic cleavage and heterolytic cleavage (Scheme 2.6). Homolytic cleavage of  $H_2$  results in a pair of hydrogen atoms, each with one electron. Heterolytic cleavage of  $H_2$  results in a proton and a hydride anion with two electrons.

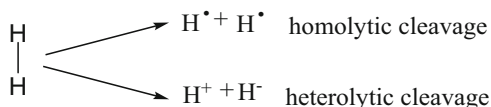
#### 2.2.1.1 Homolytic Cleavage of $H_2$

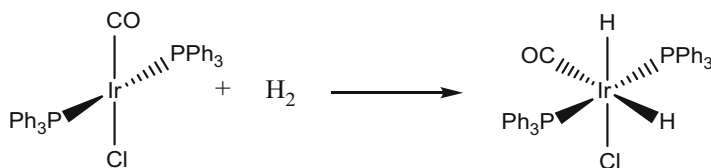
Homolytic cleavage is also referred as the model of oxidative addition of hydride to metal centers through  $H_2$  cleavage. Complexes with nucleophilic metal centers that have low oxidation states favor homolytic  $H_2$  cleavage. In homolytic cleavage, the

**Scheme 2.5** M- $\sigma$  bond for  $\eta^2$ - $H_2$  complex



**Scheme 2.6** Pathways for H–H bond cleavage

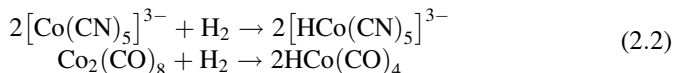




**Scheme 2.7** Homolytic cleavage of  $\text{H}_2$  by  $\text{IrCl}(\text{CO})(\text{PPh}_3)_2$

strong electron back-donation from metal center to  $\sigma^*$  orbital of  $\text{H}_2$  weakens the H–H bond; thus,  $\text{H}_2$  acts more as Lewis acid to accept electrons from  $d$  orbital of metal atom and eventually incorporate with metal center to yield metal hydride complex. Vaska made significant demonstration of homolytic hydrogen cleavage for Ir (I) complex (Vaska's compound) to yield dihydride Ir (III) complex in 1962 (Scheme 2.7) [28]. Increasing the basicity of metal center leads to stronger electron backdonation to H–H  $\sigma^*$  orbital, which further improves  $\text{H}_2$  activation (the cleavage of H–H bond). This process is essentially oxidative addition of two hydrides to the metal center, and as a consequence the oxidation state of metal center increases by two. Wilkinson's catalyst as shown in Scheme 2.4 in the introduction part is an excellent example for homolytic  $\text{H}_2$  cleavage. In this process, the crucial dihydride intermediate complex  $\text{RhClH}_2(\text{PPh}_3)_2$  is formed by rapid homolytic  $\text{H}_2$  cleavage from an unobserved dihydrogen intermediate complex  $\text{Rh}(\text{H}_2)\text{Cl}(\text{PPh}_3)_2$  [29], and the oxidation state of rhodium increases from +1 to +3. It is worth mentioning here that the oxidation state of metal can be also increased by only one instead of two in homolytic  $\text{H}_2$  cleavage. Examples are hydrogen activation by cobalt complexes,  $[\text{Co}(\text{CN})_5]^{3-}$  and  $\text{Co}_2(\text{CO})_8$ ; the oxidation state of Co in  $[\text{Co}(\text{CN})_5]^{3-}$  increases from +2 to +3, while for  $\text{Co}_2(\text{CO})_8$  increases from 0 to +1 (Eq. 2.2) with the formation of monohydride cobalt complexes instead of dihydride complexes [17]. Late transition metals ( $3d$  to  $4d$  to  $5d$ ) have more diffused  $d$  orbitals than that of early transition metals which can result in more basic metal with more  $d(\text{M})-\sigma(\text{H}^-)$  orbital overlap and thus provides stronger M–H bond. For example,  $\text{Mo}(\text{H}_2)(\text{CO})(\text{dppe})_2$  is a dihydrogen complex, while the  $\text{WH}_2(\text{CO})(\text{dppe})_2$  is a dihydride complex [30]. Another example is that  $\text{V}(\text{H}_2)\text{Cp}(\text{CO})_3$  possesses  $\eta^2\text{-H}_2$  coordination,  $\text{Nb}(\text{H}_2)\text{Cp}(\text{CO})_3$  exists in equilibrium with dihydride complex  $\text{NbH}_2\text{Cp}(\text{CO})_3$ , whereas  $\text{TcH}_2\text{Cp}(\text{CO})_3$  is a very stable dihydride complex [31].

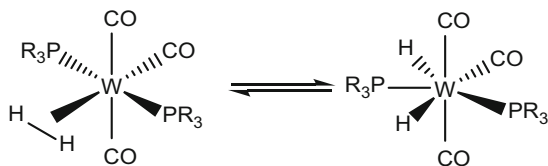
### Homolytic $\text{H}_2$ Cleavage of $[\text{Co}(\text{CN})_5]^{3-}$ and $\text{Co}_2(\text{CO})_8$



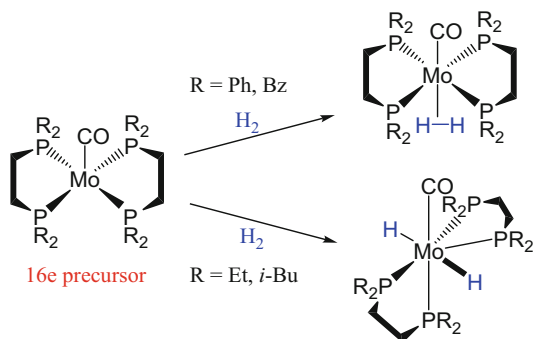
Steric effect of ligand plays a very important role in stabilizing metal dihydrogen ligand. Bulky ligand can stabilize dihydrogen ligand and inhibit the dihydrogen cleavage. Heinekey et al. synthesized  $\text{PMe}_3$  analogy of Kubas complexes  $(\text{PCy}_3)_2\text{W}(\text{CO})_3\text{H}_2$  and  $(\text{P}^i\text{Pr}_3)_2\text{W}(\text{CO})_3\text{H}_2$  ( $\text{PCy}_3$  is the tricyclohexylphosphine ligand and



**Scheme 2.8** Equilibrium existence of  $(\text{PR}_3)_2\text{W}(\text{CO})_3(\text{H}_2)$  and  $(\text{PR}_3)_2\text{W}(\text{CO})_3\text{H}_2$  in solution,  $\text{R}=\text{Cy}$  and *i*-Pr



**Scheme 2.9** Reaction of  $\text{Mo}(\text{CO})(\text{PR}_2\text{C}_2\text{H}_4\text{PR}_2)_2$  with  $\text{H}_2$



$\text{P}^i\text{Pr}_3$  is the triisopropylphosphine ligand) by photochemical synthesis [32]. By using less bulky  $\text{PMe}_3$  ligand, it has been shown that no tungsten dihydrogen complex was observed based on NMR study at various temperatures, whereas in Kubas complexes (Scheme 2.8), NMR observation confirmed the co-existence of dihydrogen complex  $(\text{PCy}_3)_2\text{W}(\text{CO})_3(\text{H}_2)$  and dihydride complex  $(\text{PCy}_3)_2\text{W}(\text{CO})_3\text{H}_2$  in equilibrium, with the domination of dihydrogen form. Another examples can be demonstrated by reaction of  $\text{Mo}(\text{CO})(\text{PR}_2\text{C}_2\text{H}_4\text{PR}_2)_2$  (where  $\text{PR}_2\text{C}_2\text{H}_4\text{PR}_2$  is a diphosphine ligand) with hydrogen; dihydrogen complex  $\text{Mo}(\text{H}_2)(\text{CO})(\text{PR}_2\text{C}_2\text{H}_4\text{PR}_2)_2$  is produced when using bulky phenyl ligand, whereas oxidative addition of two hydride ligand occurs when using smaller ethyl ligand (Scheme 2.9) [33].

Other than the nature of metal center itself, electronic effect of ancillary ligand has great influence to electron backdonation of metal center to  $\text{H}_2$  as well. Replacing electron-accepting ligand to electron-donating ligand enhances metal basicity and promotes the backdonation of M to  $\text{H}_2$  and thus causes easier  $\text{H}_2$  activation. It can also be demonstrated by  $\text{Mo}(\text{CO})(\text{PR}_2\text{C}_2\text{H}_4\text{PR}_2)_2$ . Although the size of *i*-Bu is similar to Ph,  $\text{H}_2$  cleavage occurs when using *i*-Bu ligand because  $\text{P}^i\text{Bu}_2\text{C}_2\text{H}_4\text{P}^i\text{Bu}_2$  ligand is more electron-donating than  $\text{PPh}_2\text{C}_2\text{H}_4\text{PPh}_2$  (Scheme 2.9). This ligand effect can also apply to transition metal polynuclear cluster complexes (detail will be discussed in Sect. 2.2.1.2). Some other examples for electronic and ligand effect are shown in Table 2.2 [34].

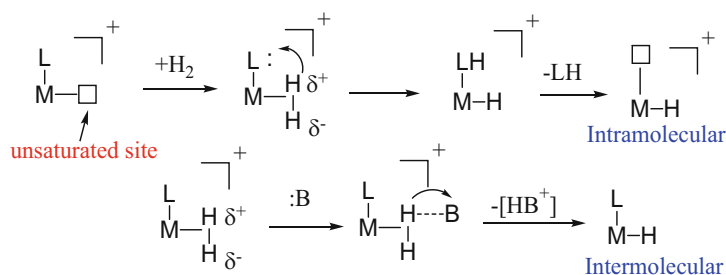
### 2.2.1.2 Heterolytic Cleavage of $\text{H}_2$

Heterolytic cleavage is a more prevalent hydrogen activation process for transition metal complexes and hydrogenase enzymes. In this process, molecular hydrogen is first polarized and splitted to hydride ion ( $\text{H}^-$ ) and proton ( $\text{H}^+$ ), resulting in the formation of metal hydride complex and protonation of an assisting Lewis donor,

**Table 2.2** Examples of effects of variation of metal, ligand, or charge on dihydrogen versus polyhydride coordination

Dihydrogen complex	Polyhydride complex
$\text{Mo}(\text{H}_2)(\text{CO})(\text{dppe})_2$	$\text{WH}_2(\text{CO})(\text{dppe})_2$
$\text{CpMn}(\text{H}_2)(\text{CO})_2$	$\text{CpReH}_2(\text{CO})_2$
$\text{TcCl}(\text{H}_2)(\text{dppe})_2$	$\text{TcH}_3(\text{dppe})_2$
$[\text{MH}(\text{H}_2)(\text{PR}_3)_4]^+$ (M=Fe, Ru)	$[\text{OsH}_3(\text{PPh}_3)_4]^+$
$\text{MH}(\text{H}_2)(\text{PR}_3)_3$ (M=Fe, Ru)	$\text{OsH}_4(\text{PR}_3)_3$
$[\text{TpOs}(\text{H}_2)(\text{PPh}_3)_2]^+$	$[\text{CpOsH}_2(\text{PPh}_3)_2]^+$
$\text{TpRuH}(\text{H}_2)(\text{PR}_3)$	$\text{CpRuH}_3(\text{PR}_3)$

depe = 1,2-bis(diethylphosphino)ethane, R = alkyl  
 dppe = 1,2-bis(diphenylphosphino)ethane, Tp = trispyrazolylborate

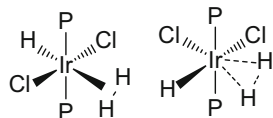


**Scheme 2.10** Two pathways for heterolytic cleavage of H<sub>2</sub>

which is a basic molecule or ligand. The assisting Lewis donor, either intramolecular basic ligand or an external basic molecule, is present to assist hydrogen cleavage by inducing polarization to H<sub>2</sub>. This eventually leads to the migration of H<sup>+</sup> to the base and the coordination of H<sup>-</sup> to metal center to form metal monohydride (Scheme 2.10). The first example of heterolytic η<sup>2</sup>-H<sub>2</sub> cleavage by cationic complex was shown by Crabtree in 1985. Cationic dihydrogen iridium complex, [IrH(H<sub>2</sub>)(PPh<sub>3</sub>)<sub>2</sub>(bq)]<sup>+</sup>, (bq = 7,8-benzoquinolato) was synthesized by treating its corresponding aquo iridium complex with hydrogen, and intermolecular heterolysis of η<sup>2</sup>-H<sub>2</sub> on [IrH(H<sub>2</sub>)(PPh<sub>3</sub>)<sub>2</sub>(bq)]<sup>+</sup> occurred by deprotonation of H<sub>2</sub> in the presence of strong external base MeLi [35].

Unlike homolytic H<sub>2</sub> cleavage, complexes with electrophilic metal center favor heterolytic cleavage of H<sub>2</sub>. The electron poor metal center has low ability to backdonate electrons to σ\* H<sub>2</sub>. Therefore, the stability of M-H<sub>2</sub> bond is determined by the electron accepting ability of both the proton acceptor from Lewis base and the metal acceptor from hydride. Increasing basicity of ligand, such as H<sub>2</sub>O or Cl ligand, can enhance the electron polarization of hydrogen and cause heterolytic cleavage of H<sub>2</sub>. For intramolecular heterolytic cleavage, basic ligand at *cis* position or close to η<sup>2</sup>-H<sub>2</sub> facilitates proton transfer. On the other hand, electron withdrawing ligand,

**Scheme 2.11**  $\text{IrCl}_2\text{H}(\text{H}_2)$   
 $(\text{PR}_3)_2$  with Cl *cis* to  $\text{H}_2$  (*left-*  
*hand side*) and Cl *trans* to  $\text{H}_2$   
*(right-hand side)*



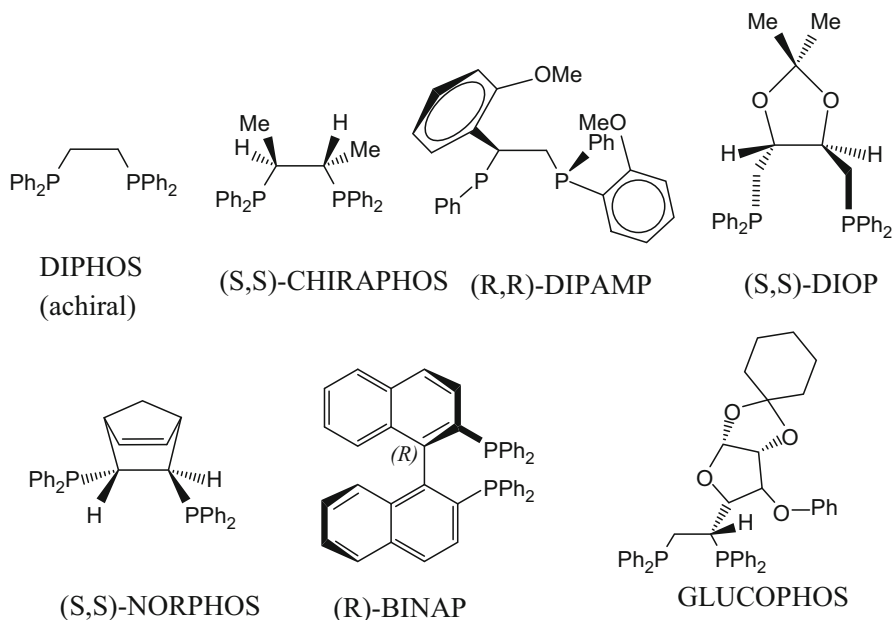
such as CO ligand, helps make metal center more electrophilic, especially at *trans* position to  $\eta^2\text{-H}_2$ ; it reduces electron backdonation of M to  $\eta^2\text{-H}_2$  greatly and thus stabilizes  $\eta^2\text{-H}_2$  coordination. Conversely,  $\sigma$  donor ligand at *trans* position weakens  $\eta^2\text{-H}_2$  coordination by reducing electron donation from  $\eta^2\text{-H}_2$  to M. The degree of  $\text{H}_2$  activation can be judged by H–H distance from X-ray or neutron diffraction and NMR coupling constant  $J_{\text{HD}}$ . This *trans* effect can be illustrated by  $\text{IrCl}_2\text{H}(\text{H}_2)(\text{PR}_3)_2$ , when Cl is in *trans* position to  $\text{H}_2$ ,  $d_{\text{HH}}$  is 0.81 Å; on the other hand,  $d_{\text{HH}}$  is 1.4 Å with Cl *cis* to  $\text{H}_2$  [36] (Scheme 2.11).

Besides the electrophilicity nature of ligand and metal, the charge of the metal center effect is another important factor to determine  $\text{H}_2$  activation. It has to be considered with ligand *trans* effect together for heterolytic  $\text{H}_2$  activation. In general, cationic metal center and electron withdrawing ligand at *trans* position greatly reduces electron backdonation and shortens H–H distance, which enhances the stability of dihydrogen complex. Strong  $\sigma$  donor ligand and neutral metal complexes favor heterolytic  $\text{H}_2$  activation. The metal charge effect can be shown by the comparison of  $\text{MoH}_2(\text{PR}_3)_5$  and  $[\text{Fe}(\text{H}_2)(\text{PH}_3)_5]^{2+}$ .  $\text{MoH}_2(\text{PR}_3)_5$  is a pure dihydride complex [37] versus  $[\text{Fe}(\text{H}_2)(\text{PH}_3)_5]^{2+}$ , which is a dihydrogen complex with very short H–H distance by theoretical calculation [38].

### 2.2.1.3 Transition Metal Complex as Homogenous Hydrogenation Catalysts

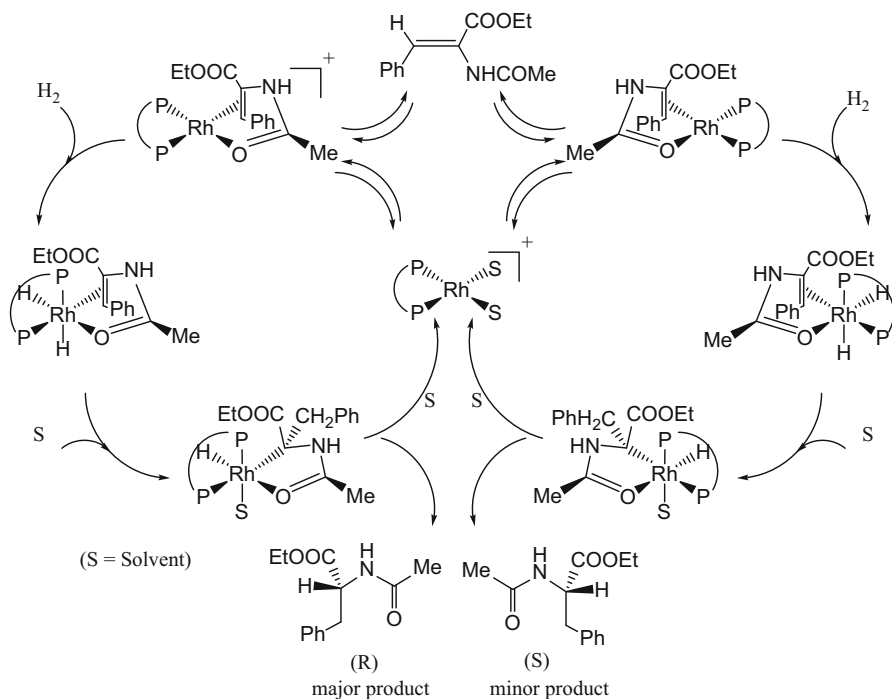
Transition metal complexes are widely used as homogenous catalysts in hydrogenation, hydroformylation [39], and hydrogen oxidation reactions to promote the activation of hydrogen [40, 41]. As stated in introduction part, Wilkinson's catalyst made an impressive example of homolytic  $\text{H}_2$  cleavage in homogenous hydrogenation reaction. James published two review articles in 1970s which thoroughly reviewed a variety of homogenous hydrogenation mononuclear transition metal complexes of earlier days.

Asymmetric hydrogenation plays a very important role in industry where high quality precise chemical synthesis is desired, such as in pharmaceuticals, fragrances, and agrochemicals. Transition metal catalysts containing chiral diphosphine ligand have been demonstrated to significantly enhance product stereoselectivity in hydrogenation reactions (Scheme 2.12) [42–44]. In the 1970s, Monsanto company developed Rh (I) complexes containing chiral diphosphine DIPAMP for asymmetric hydrogenation across unsymmetrical C=C to synthesize L-DOPA in industrial scale which is an essential drug for treatment of Parkinson's disease [45, 46]. This invention made significant milestone on the development of enantioselective



**Scheme 2.12** Structures of selected chiral diphosphines

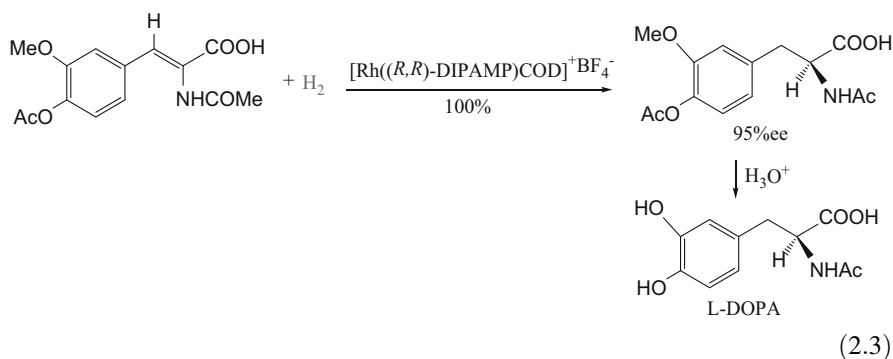
catalysis for its recognition as the first industrial asymmetric synthesis, and the inventor, William S. Knowles, shared one quarter of Nobel Prize in 2001 for his development of chiral catalyst. The asymmetric hydrogenation catalyzed by Rh-DIPAMP cation yield spectacular enantioselectivity of 95% ee (Eq. 2.3). The reaction mechanism of asymmetric hydrogenation by the Rh(I) chiral diphosphine catalyst has been demonstrated by Halpern [47] and it is the most studied mechanism for asymmetric hydrogenation. In catalytic hydrogenation cycle by Wilkinson's catalyst, which is also an Rh (I) complex (see Scheme 2.4), reversible oxidative addition of H<sub>2</sub> to form rhodium dihydride complex is involved as an essential catalytic intermediate. Such dihydride mechanism can also be applied to Rh (I) catalyzed asymmetric hydrogenation, although it is proposed that unsaturated mechanism is also suitable to explain the catalytic cycle. The difference between these two mechanisms is not practically important because the resulting stereoselectivity in the catalytic reaction is always the same [48]. Scheme 2.13 presents the mechanism of asymmetric hydrogenation of ethyl (Z)-1-acetamidocinnamate (EAC) by using Rh(I)-diphosphine catalyst. First, solvent molecules that are coordinated to Rh complex dissociate and are displaced by EAC through olefinic  $\pi$  bond and carbonyl interaction with Rh (I) center, followed by oxidative addition of H<sub>2</sub> to the Rh (I) forming Rh (III) dihydride intermediate. Subsequently,



**Scheme 2.13** Mechanism of Rh-diphosphine-catalyzed hydrogenation of ethyl (Z)-1-acetamidocinnamate (EAC)

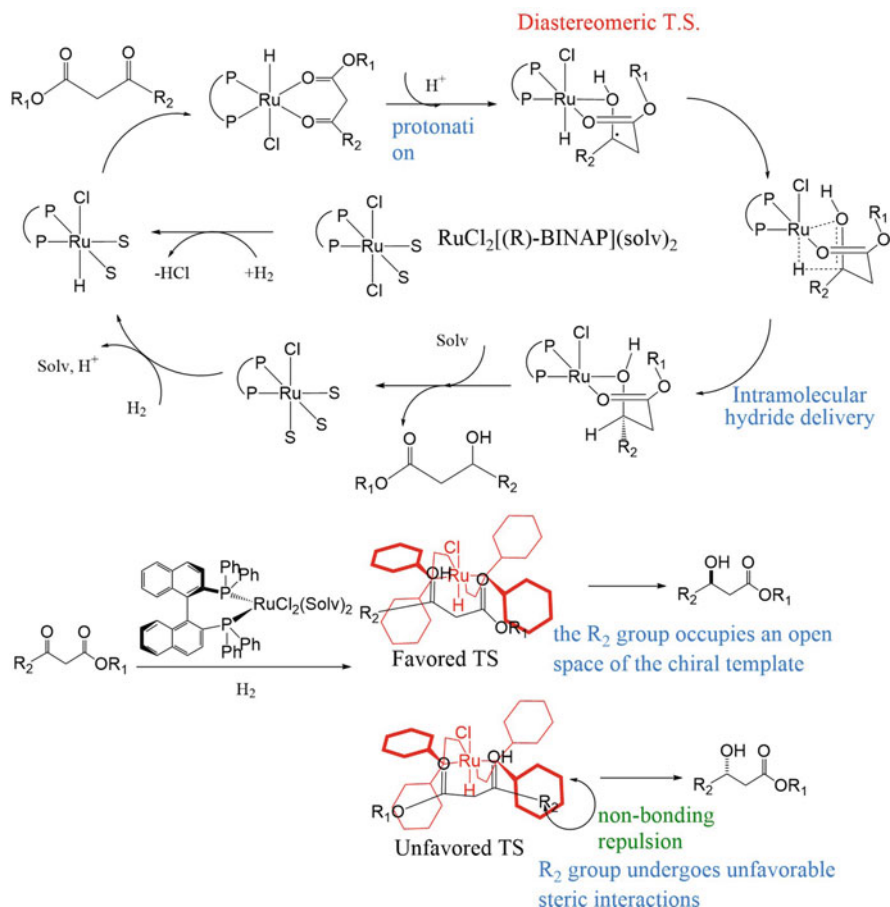
one of the hydrides on Rh (III) centers migrates to the coordinated olefinic bond to form Rh-alkyl  $\sigma$  bond with one solvent molecule coordinated back to the metal center. Final reduction phenylalanine is eliminated with the other hydride and regenerate the initial catalyst. In theory, two diastereoisomers of phenylalanine products should be produced when the chiral ligand possesses C<sub>2</sub> symmetry, because the olefin can bind to Rh complex center by either the *re* face or the *si* face at the first step in the catalytic cycle. However, practically, high enantioselectivity product of (R) enantiomer is achieved. Kinetic studies for Rh (I) CHIRAPHOS catalyst explained the reason: at the rate determining oxidative addition of H<sub>2</sub> step, the intermediates for both (R) and (S) enantiomer form rapidly, but the intermediate for (R) enantiomer is produced much faster than that for (S) enantiomer, which leads to the preference of (R) enantiomer as the major final product. Experimental studies have shown that using CHIRAPHOS ligated Rh (I) complex for asymmetric hydrogenation of methyl-(Z)-1-acetamidocinnamate also results in the same analogous enantiomer as the above with good selectivity [49] (Scheme 2.13).

### The Monsanto synthesis of L-DOPA using catalytic asymmetric chiral Rh(I) complex



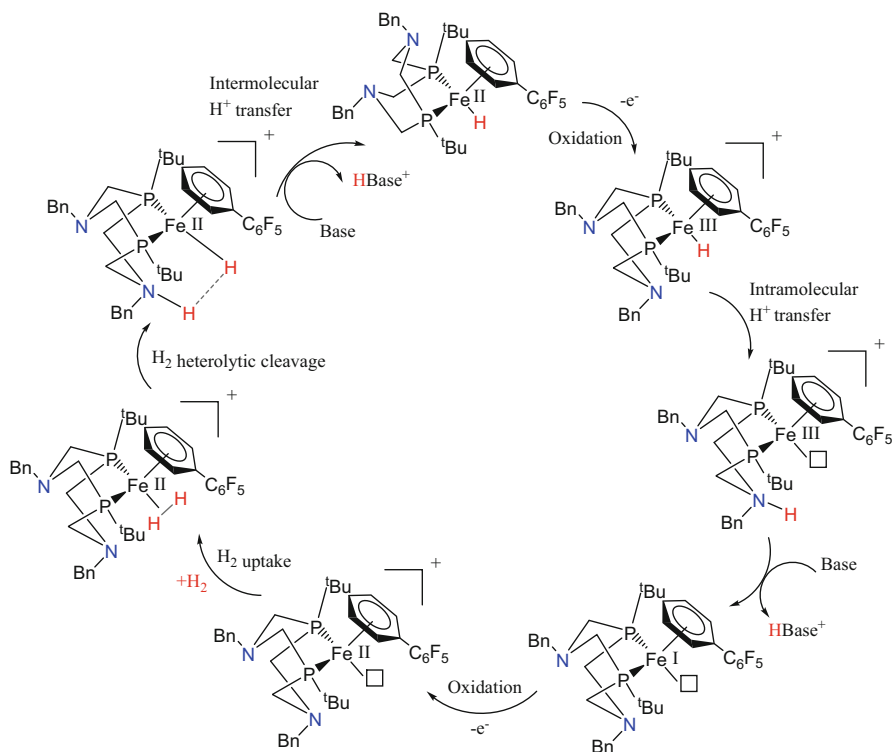
Other than Rh (I)-diphosphine complex catalysts, chiral Ru (II)-diphosphine complex catalysts, particularly Ru (II)-BINAP catalyst, are also exceptional for stereoselective organic synthesis in industry. Ru (II)-BINAP catalysts are discovered by Ryōji Noyori who is recognized as one of the Nobel Laureates in Chemistry and shared half of prize with William S. Knowles in 2001. Ryōji Noyori introduced chiral Ru catalysts for asymmetric hydrogenation of ketones, aldehydes, and imines. The Ru (II)-BINAP catalysts exhibit spectacular high stereoselectivity of asymmetric hydrogenation and the product is even predictable, depending on if (S)- or (R)-BINAP ligand is used. Example here is given for the asymmetric hydrogenation of  $\beta$ -keto carboxylic ester (Scheme 2.14). In this catalytic cycle, Ru (II)-BINAP complex first activates dihydrogen by heterolytic cleavage to form Ru-monohydride intermediate and HX by the loss of one halide ligand (X = halide). The ketone ester compound coordinates to ruthenium center with the loss of another coordinated solvent molecule. Due to the chirality of BINAP ligand, in the next step, proton transfer occurs to the carbon atom on ketone, followed by the elimination of hydrogenated ester with the coordination of solvent ligand, and the ruthenium complex can activate H<sub>2</sub> again by heterolytic cleavage to catalyze the reaction cycle [50]. Noyori made tremendous progress in improving the selectivity for the ketone hydrogenation products. Lots of scientists over the world continue investigating this type of chiral Ru catalyst for different kinds of asymmetric ketone hydrogenation.

Hydrogen oxidation reaction split molecular hydrogen into two protons and two electrons, which converts the chemical energy of H–H bond to electric energy. Among the three types of active hydrogenases, [FeFe] hydrogenases and [NiFe] hydrogenases are the most studied. The hydrogen activation reactivity is not only influenced by the organometallic active site of hydrogenase, it is also greatly affected by its surrounding enzyme matrix. The reactivity of H<sub>2</sub> activation is very sensitive to ligand selection. Inspired by the nature of biological system, scientists use the basic ligand, such as pendant amine group to facilitate proton transfer for transition metal complexes. Earth-abundant transition metals, such as Ni, Fe, Mn, are used to



**Scheme 2.14** Mechanism of Ru(II)-BINAP catalyzed substrate-directed ketone hydrogenation

catalyze hydrogen oxidation reaction. Recently, a mononuclear iron complex,  $\text{Cp}^{\text{C}_6\text{F}_5}\text{Fe}(\text{P}^{\text{tBu}}_2\text{N}^{\text{Bn}}_2)\text{H}$ , is shown to be efficient molecular catalyst for hydrogen oxidation reaction (1.0 atm, 22 °C) at the highest turnover frequencies of  $2.0 \text{ s}^{-1}$  among all iron complex catalysts reported to date (Scheme 2.15) [51]. Pendant amine group is used as  $\sigma$ -donor ligand to assist intramolecular  $\text{H}_2$  cleavage in the catalytic cycle. *Tert*-butyl groups can avoid competitive binding of exogenous amine base and favor dihydrogen coordination in the cycle. In this catalytic cycle, Fe (II)-H is first oxidized to Fe (III)-H cation complex, followed by the proton transfer to the adjacent pendant amine group. By the intermolecular deprotonation of exogenous amine base, Fe (II)-H cation is reduced to neutral Fe (I), which is then electrochemically oxidized to Fe (II) complex. Fe (II)- $\text{H}_2$  is formed as intermediate with  $\text{H}_2$  uptake, followed by  $\text{H}_2$  heterolytic cleavage, which is promoted by the pendant amine group. In the final step of this catalytic cycle, exogenous amine base



**Scheme 2.15** Proposed mechanism for electrocatalytic oxidation of H<sub>2</sub> [51]. (Bn = benzyl)

deprotonates again to complete the catalytic cycle and regenerates Fe (II)-H complex.

## 2.2.2 Heterometallic Cluster Complexes for Hydrogen Activation

### 2.2.2.1 Heterometallic Cluster Complexes for Hydrogen Activation and Homogenous Hydrogenation Catalysis

Transition metal cluster chemistry made tremendous development over the last 50 years. A metal cluster complex can be defined as the compound that contains two or more metal atoms that are held together by direct and substantial metal–metal bonds. It can serve as effective structural model to study chemisorbed process on metal surfaces, which is known as the cluster-surface analogy [25, 26]. Therefore, investigating hydrogen activation process by using metal cluster complexes is particularly of great importance for the study of heterogeneous hydrogenation catalysis. Furthermore, the characterization of cluster compounds in solution and the solid state by using spectroscopic (particularly infrared, NMR and mass spectrometry) and



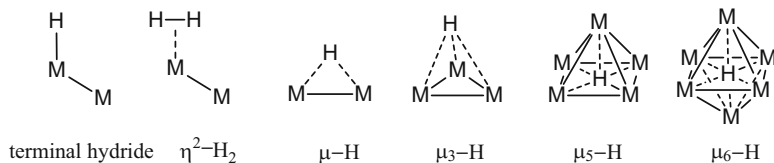


**Fig. 2.2** Hydrogen bonding mode in metal cluster complexes. Terminal hydride ( $\eta^1\text{-H}$ ) and dihydrogen side on coordination ( $\eta^2\text{-H}_2$ ) as the same with mononuclear complexes, bridging hydride with different number of metals ( $\mu\text{-H}$ ,  $\mu_3\text{-H}$ ,  $\mu_5\text{-H}$ ,  $\mu_6\text{-H}$ )

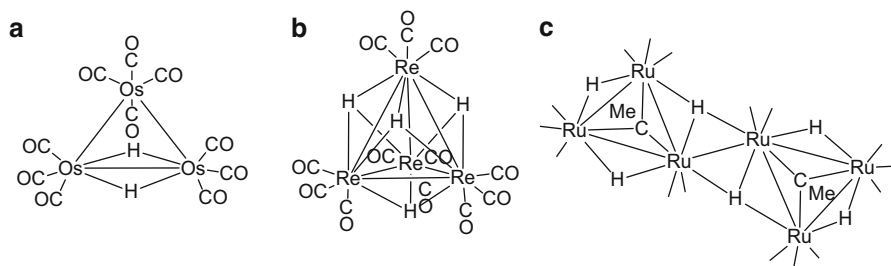
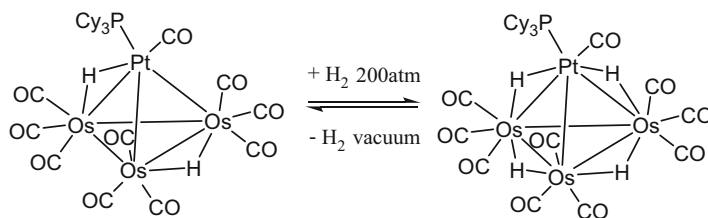


**Fig. 2.3** Examples of unsaturated polynuclear metal complexes containing bridging hydride ligands

diffraction techniques (single-crystal X-ray and neutron diffraction) can provide insightful understanding for metal surfaces at the atomic and molecular levels.

Heteronuclear metal cluster complexes include the electron-precise polyhedral cluster complexes in which all the metal atoms have the closed shell 18 electron configuration, as well as the complexes in which the metal atoms interact with each other by forming delocalized bonds that can be explained by polyhedral skeletal electron pair theory [52]. Electronic unsaturation in metal complexes captured great attention to organometallic chemists. It can be found as a vacant coordination site or metal–metal multiple bonds in cluster complexes. Any polynuclear transition metal cluster complexes that can activate hydrogen must contain vacant molecular orbital (electronically unsaturated) or undergo ligand dissociation by heat or light to generate unsaturated coordination site before interacting with hydrogen. Metal skeleton rearrangement can also provide unsaturated site during the process for hydrogen activation. In mononuclear transition metal complexes, hydrogen interacts with metal center by either coordinated hydride or side-on  $\eta^2\text{-H}_2$  (Scheme 2.2 and 2.3) [53]. In transition metal cluster complexes, hydrogen can form delocalized bonds to bridge metal atoms in a variety of bonding mode (Fig. 2.2). Delocalized hydrogen can also disguise the unsaturation of polynuclear metal cluster complexes, such as the 46-electron triosmium complex  $\text{Os}_3(\text{CO})_{10}(\mu\text{-H})_2$  [54], **A**, the 56-electron tetrarhenium complex  $\text{Re}_4(\text{CO})_{12}(\mu\text{-H})_4$  [55], **B**, and higher nuclear clusters such as the hexaruthenium carbonyl complex with 92 electrons  $[\text{Ru}_3(\text{CO})_8(\mu_3\text{-CMe})(\mu\text{-H})_2(\mu_3\text{-H})_2]$  [56], **C** (shown in Fig. 2.3). Particular detail is provided for compound **A**, which is formed by  $\text{H}_2$  addition to  $\text{Os}_3(\text{CO})_{10}(\text{NCMe})_2$  due to labile NCMe

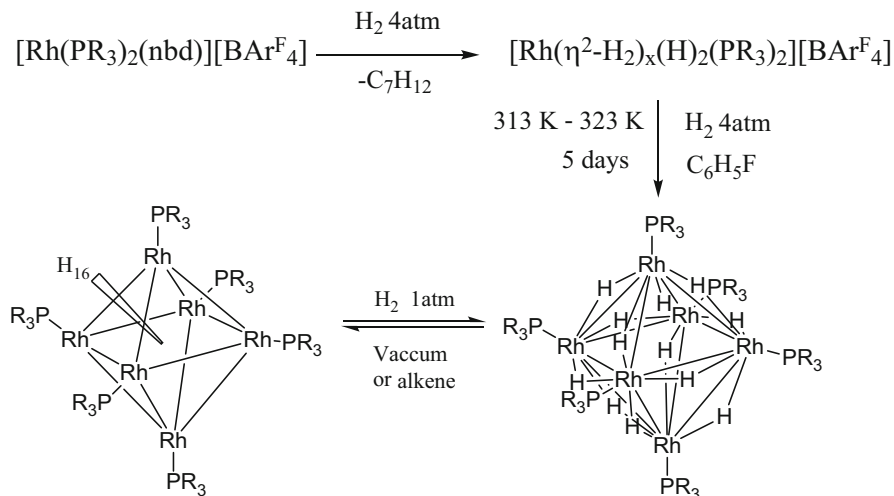


**Scheme 2.16**  $\text{PtOs}_3(\text{CO})_{10}(\text{PCy}_3)(\mu\text{-H})_2$  reacts with  $\text{H}_2$  under 200 atm to  $\text{PtOs}_3(\text{CO})_{10}(\text{PCy}_3)(\mu\text{-H})_4$ . The loss of one equivalent  $\text{H}_2$  occur upon vacuum

ligand dissociation. Many transition metal cluster complexes can interact with  $\text{H}_2$  without ligand dissociation or metal cluster rearrangement to yield metal-hydride complexes; however, some of the reactions only precede under relatively harsh condition. For example, unsaturated bimetallic cluster  $\text{PtOs}_3(\text{CO})_{10}(\text{PCy}_3)(\mu\text{-H})_2$  is two-electron short and shown to reversibly take up 1 equivalent of  $\text{H}_2$ , but this hydrogen addition requires a high  $\text{H}_2$  pressure of 200 atm (Scheme 2.16).

On the other hand, some transition metal cluster complexes readily take up hydrogen under very mild condition. Weller and coworkers have reported a series of highly electronically unsaturated hydrogen rich polynuclear metal cluster complexes,  $[\text{Rh}_6(\text{PR}_3)_6\text{H}_{12}][\text{Y}]_2$  ( $\text{R} = i\text{-Pr}$ ,  $\text{Cy}$ ;  $\text{Y} = [\text{B}\{\text{C}_6\text{H}_3(\text{CF}_3)_2\}_4]$  or 1-*H-closo*- $\text{CB}_{11}\text{Me}_{11}^-$ ), which are formed from condensation of mononuclear complex  $[(\text{R}_3\text{P})_2\text{Rh}(\text{nbd})][\text{Y}]$  ( $\text{nbd} = \text{norbornadiene}$ ) under hydrogen [57]. The structure of the  $\text{Rh}_6$  complex consists of an octahedral cluster of six Rh atoms with wide range of Rh–Rh distance 2.7181(3)–3.0597(5) Å and each of the 12 hydride ligands bridges one Rh–Rh, which is known to elongate metal–metal bond. Interestingly,  $[\text{Rh}_6(\text{PR}_3)_6\text{H}_{12}][\text{BAR}^{\text{F}}_4]_2$  ( $\text{R} = i\text{-Pr}$ ,  $\text{Cy}$ ;  $\text{BAR}^{\text{F}} = [\text{B}\{\text{C}_6\text{H}_3(\text{CF}_3)_2\}_4]$ ) is found to be capable of rapidly adding two molecules of  $\text{H}_2$  under 1 atm either in  $\text{CH}_2\text{Cl}_2$  or in crystalline form to give 16 hydride cluster complex  $[\text{Rh}_6(\text{PR}_3)_6\text{H}_{16}][\text{BAR}^{\text{F}}_4]_2$  without any metal cluster rearrangement. Upon the influence of vacuum, two hydrogen molecules dissociate from the 16-hydride complex and regenerate its 12-hydride precursor (Scheme 2.17) [58]. The resulting 16-hydride cluster is also highly unsaturated which contains 80 electrons (saturated octahedral transition metal cluster should contain 86 electrons). This is due to steric effect of bulky  $\text{PR}_3$  ligand, which acts as shield to prevent molecules from disturbing metal core except the smallest  $\text{H}_2$  and thus stabilizing the whole cluster.

Adams and Captain have shown that the 12-electron  $[\text{M}(\text{PBU}^t_3)_2]$  ( $\text{M} = \text{Pd}$  or  $\text{Pt}$ ) is an exceptional reagent that can be introduced to some transition metal carbonyl complexes to synthesize stable, highly unsaturated mix metal cluster complexes [59, 60]. The resulting polynuclear-mixed metal cluster complexes contain bulky  $\text{PBU}^t_3$  ligand to provide large steric effect to shield the metal core atoms and exhibit high reactivity for hydrogen activation. Bimetallic cluster complex  $[\text{Pt}_3\text{Re}_2(\text{CO})_6(\text{PBU}^t_3)_3]$  can be obtained from the reaction of  $\text{Re}_2(\text{CO})_{10}$  with  $\text{Pt}(\text{PBU}^t_3)_2$  in octane reflux (125 °C). The resulting complex is highly unsaturated with only 62 electrons, which is 10 electrons shorter than that of a saturated trigonal



**Scheme 2.17**  $[\text{Rh}_6(\text{PR}_3)_6\text{H}_{12}][\text{BAr}^{\text{F}}_4]_2$  ( $\text{R} = i\text{Pr}, \text{Cy}$ ;  $\text{BAr}^{\text{F}} = [\text{B}\{\text{C}_6\text{H}_3(\text{CF}_3)_2\}_4]$ ) can add two equivalents of hydrogen reversibly under very mild conditions

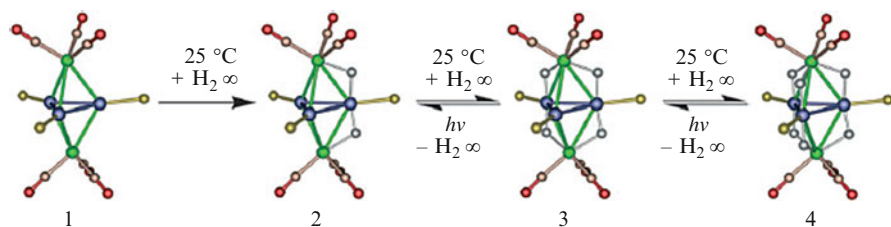


**Fig. 2.4** Reversible addition of  $\text{H}_2$  to the  $\{\text{Pt}_3\text{Re}_2\}$  cluster complex **1**. Blue Pt, green Rh, yellow P, red O, light brown C, gray H [63] (Reproduced with permission from Ref. [63]. Copyright © 2009 American Chemical Society)

bipyramidal cluster. This complex has very unusual reactivity and is capable of sequentially adding three equivalent of  $\text{H}_2$  at room temperature and reversibly eliminating two equivalent of  $\text{H}_2$  under UV irradiation (Fig. 2.4) [61]. In this process,  $\text{H}_2$  is activated and added to the metal cluster by forming hydrido ligands that bridge Pt–Re without any ligand dissociation. The mechanism for  $\text{H}_2$  addition at multiple metal centers was investigated by density functional theory (DFT) calculation, which suggests that hydrogen activation on platinum atom is more energetically favorable than on rhenium atom [62]. For the addition of  $\text{H}_2$  from **1** to **2**, computational experiment indicated that  $\text{H}_2$  activation can undergo two possibilities, both of which involve multiple metal atoms (Fig. 2.5). For the 1st pathway,  $\text{H}_2$  activation occurs on two Pt metal atoms by  $\text{H}_2$  interaction with one Pt center in a  $\eta^2\text{-H}_2$  mode as transition state, followed by heterolytic cleavage of H–H to form bridging hydrido ligand and a free hydride ligand. For the 2nd pathway, two Pt atoms and one Re

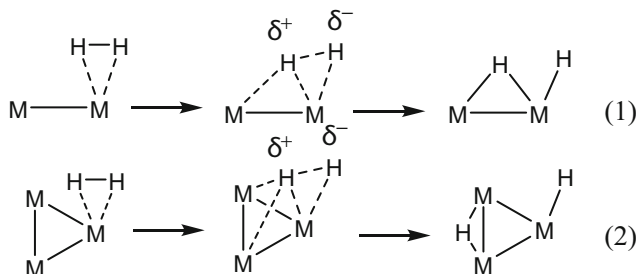
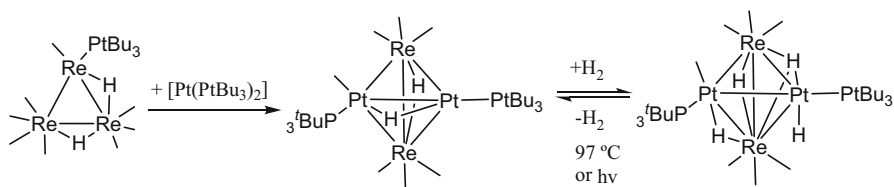


**Fig. 2.5** Schematic representation of the two-center (1) and three-center (2) activation of dihydrogen observed in the transition states



**Scheme 2.18**  $\text{Pt}_2\text{Re}_2(\text{CO})_7(\text{PtBu}^t_3)_2(\mu\text{-H})_2$  synthesis and reversible  $\text{H}_2$  addition

atoms are involved in the H–H cleavage:  $\eta^2\text{-H}_2$  is activated to form a hydrido ligand across Pt–Re bond and a terminal hydride on Pt atom through heterolytic cleavage.

Another unsaturated Pt–Re bimetallic cluster complex  $\text{Pt}_2\text{Re}_2(\text{CO})_7(\text{PtBu}^t_3)_2(\mu\text{-H})_2$  can also reversibly take up  $\text{H}_2$ . This cluster complex has only 54 electrons for the tetrahedral  $\text{Pt}_2\text{Re}_2$  core. One equivalent of  $\text{H}_2$  can be added to form  $\text{Pt}_2\text{Re}_2(\text{CO})_7(\text{PtBu}^t_3)_2(\mu\text{-H})_4$  with four bridging hydrido ligand at room temperature 1 atm and can be eliminated under high temperature or UV irradiation (Scheme 2.16). Late transition metals, such as Pt, Pd, Rh, Ir, tend to initiate hydrogen activation in transition metal cluster complexes. Computational method indicated the heterolytic cleavage of  $\text{H}_2$  that involved multiple metal atoms. These transition metal cluster complexes have low lying lowest unoccupied molecular orbital (LUMO) that readily take up two electrons from hydrogen molecule (Scheme 2.18).

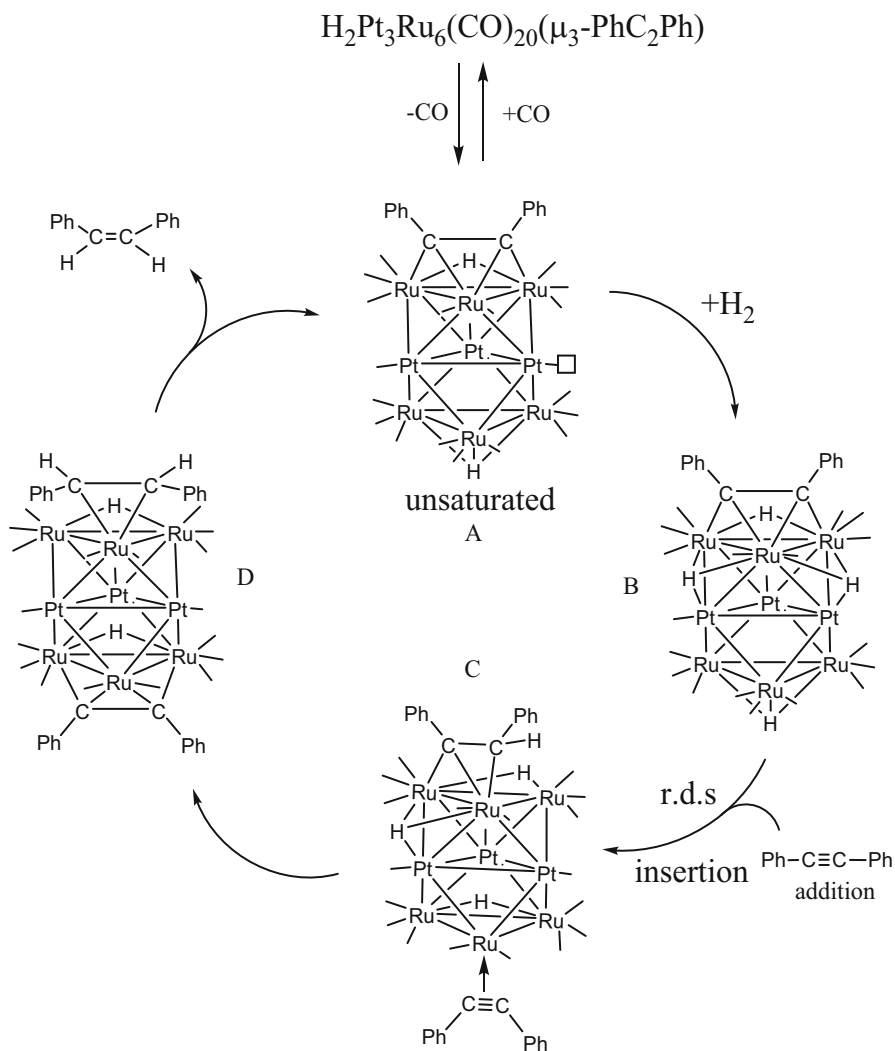
Moreover, transition metal carbonyl cluster complexes exhibit superior properties as homogeneous hydrogenation catalysts. Although in some metal cluster catalytic system, it is indeed the mononuclear metal fragment, which is formed after the loss of ligands from the cluster that actually acts as the catalysts; [64] there are still some examples where catalysis is achieved by intact clusters complexes. In the homogeneous metal cluster catalyzed hydrogenation reaction, one or more metal atoms in the cluster can serve as an active site to convert the reactants into products, and the cluster catalyst is an integral part of the catalytic cycle. For example, the complex  $\text{Pt}_3\text{Ru}_6(\text{CO})_{20}(\mu_3\text{-PhC}_2\text{Ph})(\mu_3\text{-H})(\mu\text{-H})$  has been shown to be an effective catalyst for the hydrogenation of diphenylacetylene to (*Z*)-stilbene under mild condition [65]. In this layer segregated metal cluster complex, the central triangular layer contains

three platinum atoms, while each of the two outer triangle layers contains three ruthenium atoms. Kinetic study showed that the rate of (Z)-stilbene formation is inverse first-order function with respect to the CO pressure which indicated the CO ligand dissociation must be involved to initiate the catalytic cycle. Mechanism of this hydrogenation reaction was proposed, see Scheme 2.19. An electronically unsaturated cluster complex **A** was the active catalytic species formed by the dissociation of one CO ligand at Pt atom, followed by the activation of H<sub>2</sub> to a proposed complex **B** with four hydrido ligand. And then alkyne was inserted to the cluster complex, which is the rate determination step (r.d.s) because it was demonstrated that (Z)-stilbene formation was first-order dependent on alkyne concentration. Bridging hydrido ligands were transferred to hydrogenate alkyne which was then eliminated to reform the active species **A**. The formation of (Z)-stilbene was observed at a turnover frequency of 47 h<sup>-1</sup>, suggesting the effective catalytic property of Pt<sub>3</sub>Ru<sub>6</sub>(CO)<sub>20</sub>(μ<sub>3</sub>-PhC<sub>2</sub>Ph)(μ<sub>3</sub>-H)(μ-H) as a homogenous hydrogenation catalyst (Scheme 2.19).

### 2.2.2.2 Biomimetic Model Complexes for Hydrogen Activation

Hydrogenases are enzymes to catalyze reversibly hydrogen activation to proton and electron (Eq. 2.1). The prosthetic group of hydrogenase is an iron-sulfur cluster as shown in Fig. 2.6. The Fe<sub>4</sub>S<sub>4</sub> “Cubane” cluster is attached directly to one of the Fe atoms through a cysteine thiol bridge. This is believed to be the most possible structure of the active site with one CN<sup>-</sup> and CO on each Fe and a bridging CO on the Fe–Fe bond. The Fe–Fe bond (2.6 Å) is a typical Fe–Fe distance in dithio-bridged organometallic Fe–Fe compounds. It is worth to note that the two sulfur atoms are connected through a three-atom bridge, the middle atom is identified as nitrogen and the other two are carbon atoms. This secondary amine group is very important as it participates in the di-hydrogen activation process, namely heterolysis of H<sub>2</sub>. The “Cubane” cluster acts as electron donor in the redox process. The cyanide groups are strong electron donating ligands, which helps to stabilize the oxidized form of the di-iron unit. The coordinated water molecule is also very important, since in the hydrogen activation reactions, the coordinated water molecules have to be completely replaced by dihydrogen molecules. If the water is replaced by a CO ligand, the iron-sulfur cluster will lose its hydrogen activation capability, as CO is much stronger ligand compared to water and dihydrogen and it is impossible for dihydrogen to replace coordinated CO.

The dihydrogen activation on such a cluster has been well studied. Although numerous mechanisms have been derived along the way, the key steps of dihydrogen activation process are somewhat similar. As illustrated in Scheme 2.20, the dihydrogen activation and hydrogen production can reversibly occur on [FeFe] hydrogenase. Taken into account the dihydrogen activation as an example, under hydrogen atmosphere, the hydrogen molecule competes with the coordinated water molecule to coordinate to one of the iron atoms. The H–H σ-bond donates its two bonding electrons to the iron open site to form an agostic interaction. The dihydrogen is then quickly split between the acid (the iron atom) and base (the amino group) through a heterolytic cleavage. This intermediate is neutral. In the next



**Scheme 2.19** Proposed mechanism for the catalytic process of hydrogenation of diphenylacetylene to (Z)-Stilbene by use of  $\text{Pt}_3\text{Ru}_6(\text{CO})_{20}(\mu_3\text{-PhC}_2\text{Ph})(\mu_3\text{-H})(\mu\text{-H})$  complex as catalyst. CO ligands are omitted for clarity

step, the proton on the amine group is pumped away through the protein channel, which leaves the H-Fe-Fe as an anion. As stated above, the Cubane  $\text{Fe}_4\text{S}_4$  is an electron shuttle, which can provide electrons or take electrons away from the  $\text{H}_2$ ases. In this scenario, the Cubane takes two electrons away from the cluster and resulted in the formation of a cationic Fe-Fe cluster. The terminal hydride, at the same time, migrates to the bridging position to stabilize the oxidized metal centers. There are two pathways from the cationic intermediate, again between the competing

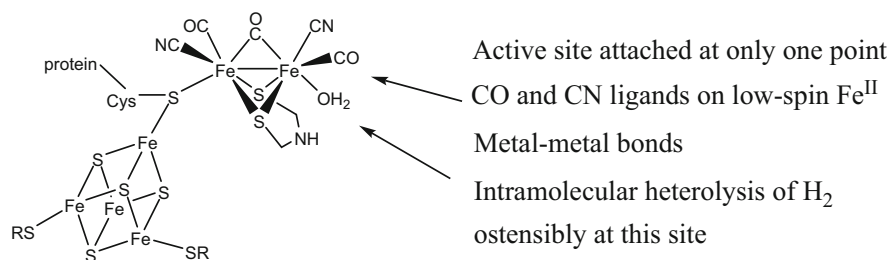
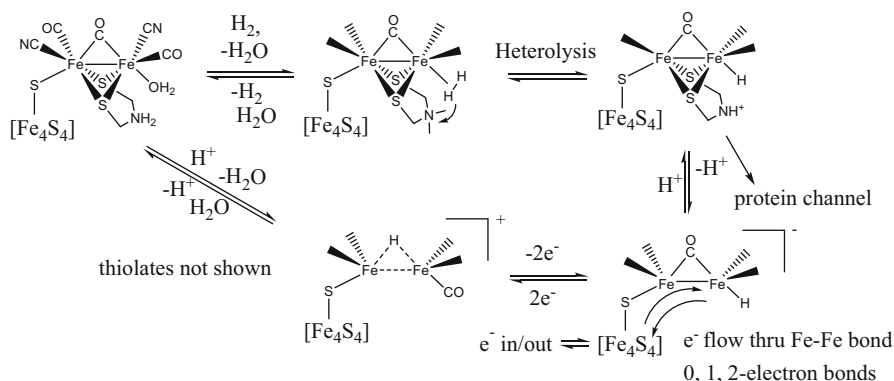


**Fig. 2.6** The prosthetic group of hydrogenase is an iron-sulfur cluster



**Scheme 2.20** Hydrogen activation and hydrogen production mechanism on [FeFe]hydrogenase

coordination of hydrogen and water molecules. The cleavage of the proton results in an open iron coordination site, which is either occupied by a water molecule to generate the original H<sub>2</sub>ases or occupied by a dihydrogen to form the H<sub>2</sub> bonded (agostic interaction) Fe–Fe cluster to complete the catalytic cycle (Scheme 2.20).

Compared to the Fe only hydrogenase, the structure of the [NiFe]hydrogenase is quite different. The structure was obtained by protein X-ray crystallography from sulfate-reducing bacteria. In combining with infrared spectroscopic analyses, the active site on [NiFe]hydrogenase was found to be (S-Cys)<sub>4</sub>Ni(μ-X)Fe(CO)(CN)<sub>2</sub> (Fig. 2.7a). It consists of heteronuclear Fe and Ni atoms, which are held together by two μ-S-cysteines bridged ligands (π-donors) and a third bridging ligand of a hydride, hydroxide, or hydroperoxide. The distance between two metal atoms ranges from about 2.9 Å for the oxidized state to about 2.5 Å for the reduced state of [NiFe]hydrogenase [66–68]. Iron atom presents the similar coordination environment as Fe(CO)(CN)<sub>2</sub> with [FeFe]hydrogenase but with two cyanide ligands. The iron remains its oxidation state at +2 and a low spin (S = 0) system, while the actual redox active site is nickel site, which is additionally coordinated to two terminal S-cysteines ligands. The oxidation state of Ni changes between +2 and +3 in its various redox forms of enzyme. It is believed that dihydrogen binding occurs on Ni site in [NiFe]

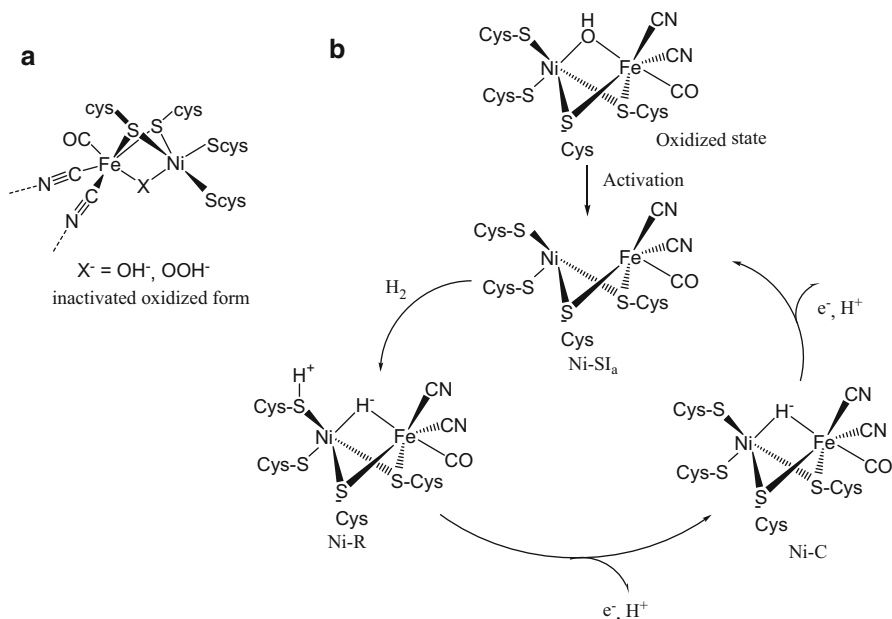


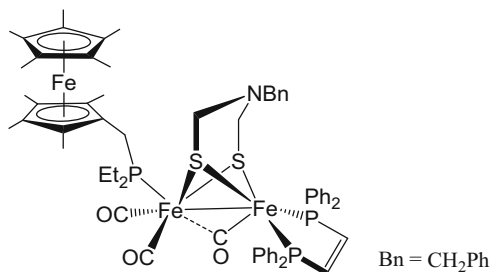
**Fig. 2.7** (a) Drawing of the active site of [NiFe]hydrogenase. (b) Proposed catalytic reaction mechanism of [NiFe] hydrogenase

hydrogenase, due to the fact that CO inhibition binds at the open site of Ni [69] and Ni position presents just at the end of H<sub>2</sub> transfer channel [70]. However, controversy has arisen from DFT calculation which suggests that Fe site is where dihydrogen binding occurs, because the vacant coordination site of  $d^6$  Fe favors direct binding of dihydrogen [71]. Recently, DFT calculation revealed that both coordination geometry and the spin state of Ni affect hydrogen activation efficiency in [NiFe]hydrogenase [72]. Regardless of the dihydrogen binding position, heterolytic cleavage leads to the formation of one bridging hydride and a proton bonded to one terminal cysteines ligand [73]. The [NiFe]hydrogenase can reversibly activate hydrogen as metal catalyst. Several redox states of Ni present as intermediates in the catalytic cycle. First, it is activated by the cleavage of bridging X ligand to form activated reduced state known as Ni-SI<sub>a</sub>, and the dihydrogen is heterolytic cleaved to form Ni-R state with a bridging hydride and proton on terminal cysteines ligand. Nickel is then oxidized to +3 oxidation state by losing one electron and yields Ni-C state accompanying by the loss of proton on the terminal cysteines ligand. The bridging hydride ligand between Fe and Ni atoms in this state was confirmed by electron paramagnetic resonance (EPR) techniques [74, 75]. Catalytic cycle is complete by further loss of hydride to yield back to Ni-SI<sub>a</sub> state (Fig. 2.7b).

Inspired by the beauty of bio-system, chemists have been making great effort on synthesizing functional models of [FeFe]hydrogenase and [NiFe]hydrogenase active site to mimic their excellent hydrogen activation and production [76–78]. Hundreds



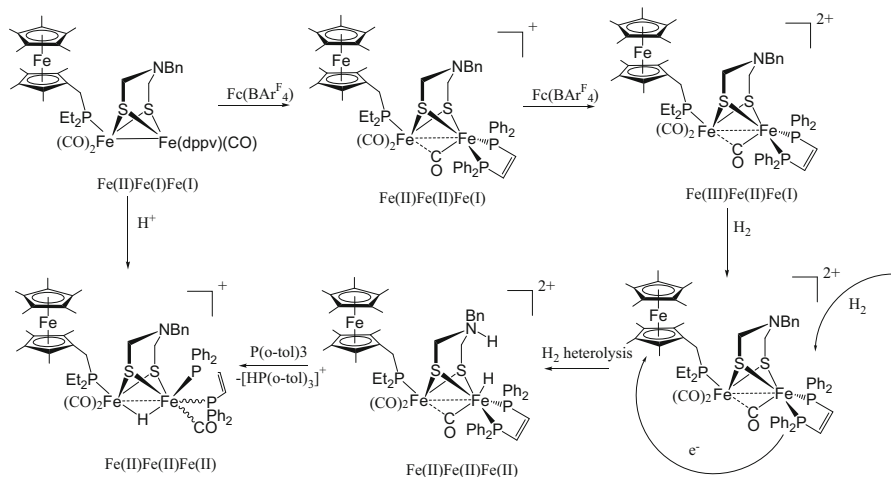
**Fig. 2.8** Drawing of the synthetic model complex  $\text{Fe}_2[(\text{SCH}_2)_2\text{NBn}](\text{CO})_3(\text{FcP}^*)(\text{dppv})$



of papers have been published regarding this subject, among which the majority are associated with  $[\text{FeFe}]$ hydrogenase and di-iron complexes. For example, recently Rauchfuss and Camara made significant progress on modeling the structural feature of  $[\text{FeFe}]$ hydrogenase by incorporating redox active ligand  $\text{Cp}^*\text{Fe}(\text{C}_5\text{Me}_4\text{CH}_2\text{PEt}_2)$  (called  $\text{FcP}^*$ ) to catalyze  $\text{H}_2$  oxidation in the presence of oxidant and base (Fig. 2.8) [79]. The  $\text{FcP}^*$  ligand simulates the function of the  $\text{Fe}_4\text{S}_4$  cluster, and it is stable in two oxidation state both at Fe (II) and Fe (III). The coordination environment of the distal iron is also very crucial for hydrogen activation. It consists of square pyramidal geometry of iron with dithiolate, diphosphine, and CO ligands, which makes the coordination site that locates at opposite side of CO ligand to be available for  $\text{H}_2$  binding.  $\text{FcBAR}^{\text{F}}_4$  is used as oxidant to oxidize ferrocenyl group from Fe (II) to Fe (III) and di-iron unit from  $\text{Fe}(\text{I})\text{Fe}(\text{I})$  to  $\text{Fe}(\text{I})\text{Fe}(\text{II})$ .  $\text{H}_2$  is uptaken and heterolytic cleaved by dication  $[\text{Fe}_2[(\text{SCH}_2)_2\text{NBn}](\text{CO})_3(\text{FcP}^*)(\text{dppv})]^{2+}$ , followed by electron redistribution to +2 oxidation state for two distal iron and ferrocenyl group. Excess  $\text{P}(\text{o-tolyl})_3$  is also provided to remove hydride on NBn, meanwhile bridging CO ligand is cleaved and coordinates to distal Fe in a terminal fashion with the formation of  $[(\mu\text{-H})\text{Fe}_2[(\text{SCH}_2)_2\text{NBn}](\text{CO})_3(\text{FcP}^*)(\text{dppv})]^+$  (Scheme 2.21).

### 2.3 Supported Nanoclusters for Hydrogenation Reactions

Heterogeneous catalytic hydrogenations are most important reactions in many industrial processes, which accounts for 10–20% reactions to produce chemicals, such as the production of pharmaceuticals, naphtha reforming for petrochemicals. Heterogeneous catalysts are used over homogeneous catalysts in industry because of their high recyclability and low cost. Supported metal catalysts are of importance in heterogeneous catalysts, for which the catalytic active metals are anchored on solid supports (such as organic polymers and inorganic oxides) or entrapped in zeolite. These supported metal catalysts often incorporate a second catalytic metal forming supported bimetallic cluster catalysts to enhance catalytic properties. The presence of two metal species can improve product selectivity, enhance the catalyst lifetime, and increase catalytic activity [80]. The catalytic performance improvement is achieved by cooperative interactions between the different metal species, which is known as synergistic effect [81]. Platinum group metal containing bimetallic



**Scheme 2.21** Hydrogen activation process for  $\text{Fe}_2[(\text{SCH}_2)_2\text{NBn}](\text{CO})_3(\text{FCP}^*)(\text{dppv})$  [79]

catalysts are extensively used in petroleum reforming for converting low-octane rating petroleum naphtha to high-octane gasoline [82–85]. The first bimetallic catalyst in industry for petroleum reforming is alumina-supported Pt–Re catalysts in 1969 [86, 87]. Later alumina-supported Pt–Ir and Pt–Sn bimetallic catalysts were discovered to exhibit superior catalytic properties compared to monometallic Pt catalysts [88]. The catalytic species are generally much smaller in size (average size 10–50 Å) and dispersed on the support compared to bulky metals. Especially in supported bimetallic catalysts, some of metals can form alloy-like nanocluster when they are small in size, rather than form bulky metal alloy in large scale. Catalytic activity is substantially affected by the size of the supported bimetallic catalysts. It is expected that the difference between bulky and small size bimetallic catalysts increases with decreasing of the particle size [89, 90]. Herein, only supported nanoclusters with particles size smaller than 10 Å are discussed. These nanoclusters typically contain less than 10 metal atoms, which can be considered as good models to investigate the influence of cluster structure to catalytic properties. Only heterogeneous hydrogenation reactions will be exhibited as examples to demonstrate the catalytic performance of supported nanocluster catalysts.

The most commonly used and inexpensive method for the synthesis of supported nanocluster catalysts is incipient wetness impregnation. The metal precursors are dissolved in aqueous or organic solvents, and catalyst support with the same pore volume as the metal precursor's solution is then mixed. Afterwards, the mixture is dried or calcined at elevated temperature to remove solvent, resulting in supported bimetallic catalysts with active metal species on the surface of support [91–93]. This is the simplest method and does not require any complex equipment. However, compared to supported nanocluster catalysts, the bimetallic particles made from this method are relatively large forming alloy species. Besides, the interaction of

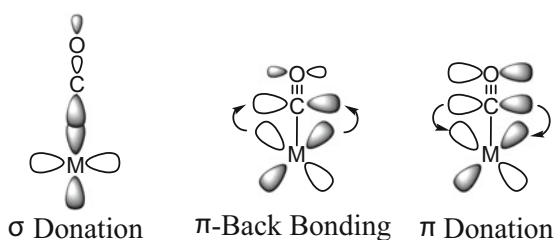
difference metal precursors is not strong enough to form uniform bimetallic species during deposition, so that it is difficult to identify the precise structure of bimetallic particles prepared from incipient wetness impregnation [94].

Controlled synthesis of supported bimetallic catalysts is highly desired so that the structures of bimetallic species and their influence on the catalytic property can be investigated. It is anticipated that stronger interaction between two metals significantly influence catalytic property compared to supported monometallic catalyst. By using molecular transition metal cluster complexes as precursors to prepare bimetallic cluster catalyst, the bimetallic interaction can be maximized and measured. Metal–metal bonds are “premade” before deposition on the solid support. These transition metal cluster complexes (most with carbonyl ligands) precursors have been demonstrated as excellent candidates for hydrogen activation, which is an essential step in hydrogenation reaction.

### 2.3.1 Transition Metal Cluster Complexes as Precursors for Heterogeneous Hydrogenation

Transition metal carbonyl complexes contain carbonyl ligands that bond terminally to one transition metal atom or coordinate to two or more transition metal atoms in a bridging fashion. The transition metal–carbonyl bonding interaction involves  $\sigma$ -bonding of the CO ligand to the empty  $d$  orbital of the transition metal, as well as the  $\pi$  back bonding from a filled metal  $d$  orbital to an empty  $\pi^*$  orbital of CO ligand (Fig. 2.9). The CO ligand has a high tendency to stabilize metal–metal bonding in cluster complexes due to the capability of CO ligand to reduce electron density on the metal through  $\pi$ -backbonding. The first metal carbonyl complex,  $\text{Ni}(\text{CO})_4$ , was discovered by Ludwig Mond in 1890, which is an intermediate used to produce pure nickel metal by the Mond process [95]. Transition metal cluster complexes used as homogenous and heterogeneous catalysts have drawn significant attention to chemists since 1960s [96]. Mix-metal cluster complexes not only can be used as homogenous catalysts in organic solution (Sect. 2.2.2.1), due to the synergism among multiple catalytic systems derived from mix-metal centers, they can also be used in heterogeneous catalytic system in which metal cluster derived particles are anchored on solid supports. Many transition metal cluster complexes have been shown to serve as precursors to generate heterogeneous catalysts for a variety of

**Fig. 2.9** The bonding between a terminal carbonyl ligand and transition metal atom



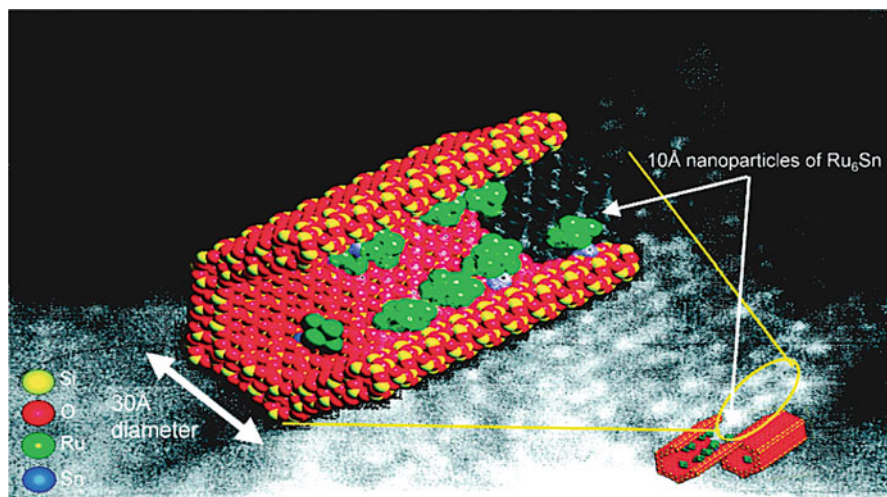


**Fig. 2.10** Computer graphic illustration of  $\text{Ru}_6\text{Sn}$  nanoparticles encapsulated on the inner surface of silica on an enlarged SEM image of the same system (Reproduced with permission from Ref. [97]. Copyright © 2003 American Chemical Society)

important industrial processes [97, 98], such as petroleum reforming, hydrogenation, and dehydrogenation reactions. There are several advantages to use transition metal cluster complexes as precursors to make heterogeneous catalysts.

1. Heterogeneous catalysis is a surface phenomenon which is greatly influenced by interaction between reactant species and catalyst. Intensive efforts have been made to reduce the size of the heterogeneous catalysts to nanoscale so that metal catalysts can be more finely dispersed which can significantly improve the catalytic efficiency. Transition metal cluster complexes are limited in size. Most of the metal cluster complexes contains less than ten metal atoms. Highly condensed metal cluster is also found, such as palladium clusters  $\text{Pd}_{69}$  [99], and  $\text{Pd}_{145}$  [100], for which the diameters are in nanometer scale and have close-packed frameworks described as *cpc* (cubic close-packed) stacking layers. These cluster complexes have been considered as proper model for the study of very small transition metal particles and metal surface chemisorption on heterogeneous catalysts [101]. Particularly for transition metal carbonyl complexes in which the transition metals are in low oxidation states, the carbonyl ligands can be readily removed under thermal treatment which also makes the resulting bare clusters to anchor firmly on the oxide support (Fig. 2.10). The resulting bare cluster catalysts are very small in size with more surface to volume ratio, therefore provide better catalyst exposure to the reactant species, and improve the catalytic activity. Moreover, the firm attachment of bare cluster to oxide support can significantly minimize the catalyst coalesce and sintering, and thus increase catalysts lifetime and reduce the cost.

**Table 2.3** List of metal couples in molecular mixed-metal clusters used as precursors to heterogeneous catalysts

Catalyzed reactions	Supported bimetallic cluster catalyst	
Hydrogenation of C–C multiple bonds	Ta–Rh, Ta–Ir	
	Mo–Fe, Mo–Ru, Mo–Co, Mo–Rh, Mo–Ir, Mo–Ni, Mo–Pd, Mo–Pt	
	W–Fe, W–Co, W–Ni, W–Pt	
	Fe–Ru, Fe–Co	
	Ru–Os, Ru–Co, Ru–Ni, Ru–Pd, Ru–Pt, Ru–Cu, Ru–Ag	
	Os–Ni	
	Co–Rh, Rh–Pt	
	Pt–Cu, Pt–Au	
	Hydrogenation of CO and CO <sub>2</sub>	Cr–Ru, Cr–Co, Cr–Pt
		Mo–Fe, Mo–Ru, Mo–Os
Mo–Co, Mo–Rh, Mo–Ni		
W–Os, W–Rh, W–Ir, W–Pt		
Mn–Fe, Mn–Ru, Mn–Co, Re–Os		
Fe–Ru, Fe–Os		
Fe–Co, Fe–Rh, Fe–Ir, Fe–Pd, Fe–Pt		
Ru–Os, Ru–Co, Ru–Rh, Ru–Ni		
Hydrogenation of aldehydes and ketones	Os–Rh, Os–Ni, Co–Rh, Co–Cu	
	Mo–Co, Mo–Rh, Ru–Pt	
	Os–Ni, Co–Cu, Co–Zn	

- Various characterization techniques can be applied to metal carbonyl complexes to confirm the well-defined structure (discussed in Sect. 2.2.2.1). Furthermore, for mix-metal carbonyl cluster complexes, the stoichiometry of different metal species can be guaranteed from cluster synthesis and the integrity of clusters still retained when undergo decarbonylation process to make supported nanocatalyst. The structural information and dispersion of bare metal clusters on oxide support at atomic level can be determined by X-ray absorption spectroscopy (EXAFS: extended X-ray absorption fine structure), high resolution electron microscopy, etc. By comparison, conventional incipient wetness impregnation method cannot guarantee the uniform dispersion and integrity of mix metal stoichiometry due to weak interaction of the precursors.
- Heterogeneous catalysis is more prevalent in industry than homogenous catalysis. It has been long established that bimetallic catalysts exhibit superior catalytic performance than that of monometallic catalysts in petroleum industry. Using bimetallic cluster complexes as heterogeneous catalyst precursor can provide a deeper insight into such synergistic effect due to the fact that cluster complexes contain direct metal–metal bond can be better characterized at the atomic and molecular level [102–105]. A list of the different supported bimetallic cluster catalysts used for the catalysis of various hydrogenation reactions is given in Table 2.3. A comprehensive review for the catalytic performance of each

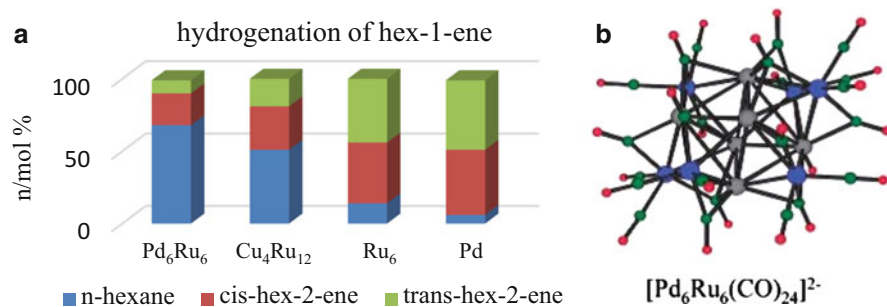


**Fig. 2.11** (a) Bar chart summarizing the relative performances and selectivities of the Pd<sub>6</sub>Ru<sub>6</sub> and Cu<sub>4</sub>Ru<sub>12</sub> catalysts when compared to monometallic Ru<sub>6</sub> and Pd nanocatalysts for the hydrogenation of hex-1-ene. (b) Parent anionic metal carbonyl complex from naked Pd<sub>6</sub>Ru<sub>6</sub> nanoparticle (17 Å diameter for the bimetallic core catalysts) (Reproduced with permission from Ref. [97]. Copyright © 2003 American Chemical Society)

supported bimetallic catalyst is given in a review article published by Buchwalter Rosé, and Braunstein recently [106]. A few examples of supported ruthenium and palladium bimetallic nanocatalysts are provided in this book chapter. Thomas and Johnson et al. [107] have reported alkene hydrogenation catalyzed by bimetallic Pd-Ru and Cu-Ru nanoparticles, which were prepared from mix-metal carbonyl cluster complexes [Pd<sub>6</sub>Ru<sub>6</sub>(CO)<sub>24</sub>]<sup>2-</sup> and [Ru<sub>6</sub>C(CO)<sub>6</sub>Cu<sub>2</sub>Cl]<sup>2-</sup>, respectively. The prepared nanocatalysts are uniformly dispersed nanoparticles, about 1.5 nm in diameter. The metal oxide loaded nanocatalysts were prepared by making a slurry of corresponding metal clusters in diethyl ether and methylene chloride with oxide support, such as mesoporous silica MCM-41 (pore size is approximately 3.0 nm), followed by activation of the encapsulated clusters upon heating at about 200 °C in vacuo. Structural retention of the clusters was confirmed by EXAFS showing the unchanged metal–metal bond. The hydrogenation of hex-1-ene, dodec-1-ene, and naphthalene were performed using these bimetallic PdRu and CuRu nanocatalyst with the comparison of individual monometallic Pd and Ru catalyst. The results of this catalytic hydrogenation of hex-1-ene are shown in a column chart in Fig. 2.11; the bimetallic nanocatalyst are much superior compared to monometallic Ru and Pd nanocatalysts for n-hexane selectivity. Also, the TOF (Turnover Frequency) for Pd<sub>6</sub>Ru<sub>6</sub> and Cu<sub>4</sub>Ru<sub>12</sub> is 20 and 10 times more than that of Ru and Pd catalysts, respectively.

Thomas and Johnson demonstrated significantly that a number of anchored bimetallic nanocatalysts generated from cluster complexes exhibit high catalytic activity and product selectivity for a series of single-step hydrogenation under low temperature (353–373 K). These are efficient hydrogen activation processes, which featured direct hydrogenation in only one step. Some of the industrial essential organic compounds have been demonstrated to be made by hydrogenation in a single step. Such catalytic reactions are desired in industry to address

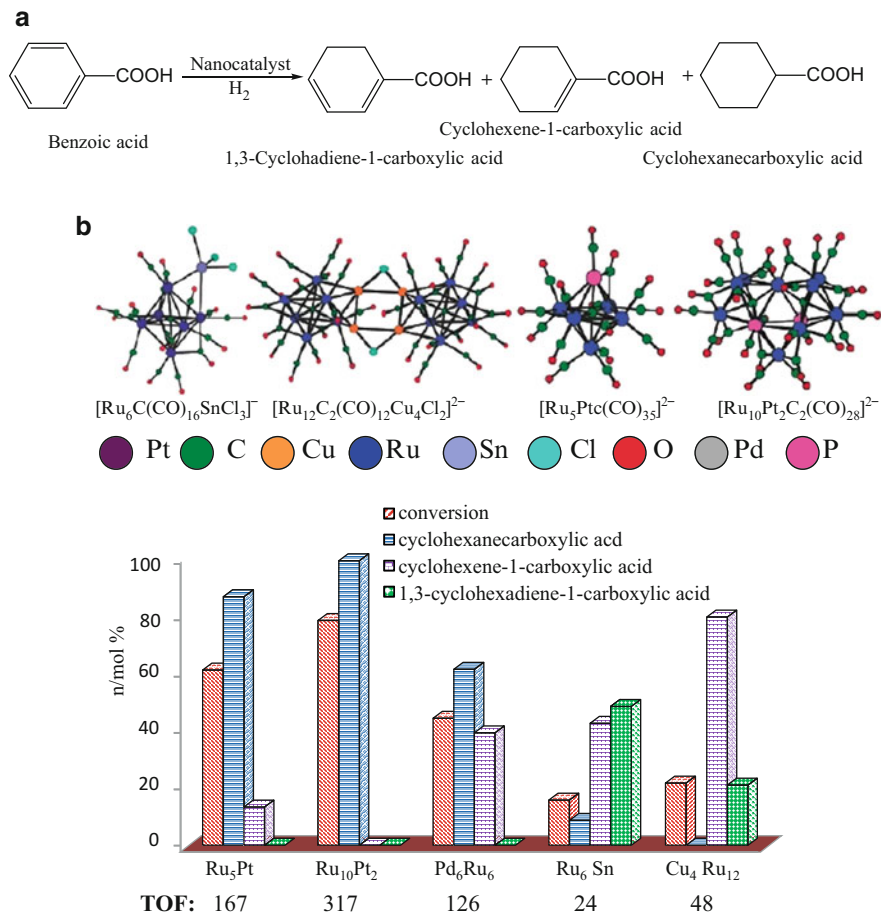


**Fig. 2.12** (a) The products from the hydrogenation of benzoic acid. (b) Parent anionic metal carbonyl complex from naked  $\text{Ru}_5\text{Pt}_1$ ,  $\text{Ru}_{10}\text{Pt}_2$ ,  $\text{Ru}_6\text{Sn}$ , and  $\text{Cu}_4\text{Ru}_{12}$  nanocatalysts nanoparticle, and bar chart summarizing the relative performances and selectivity of the  $\text{Ru}_5\text{Pt}$  and  $\text{Ru}_{10}\text{Pt}_2$  catalysts when compared to other bimetallic nanocatalysts for the hydrogenation of benzoic acid. Reaction conditions: benzoic acid: 2.5 g; catalyst, 50 mg;  $\text{H}_2$  pressure, 20 bar; Solvent:  $\text{C}_2\text{H}_5\text{OH}$  75 mL; temperature 373 K; time 24 h; TOF =  $[(\text{mol}_{\text{subst}})(\text{mol}_{\text{cluster}})^{-1} \text{h}^{-1}]$  (Reproduced with permission from Ref. [97]. Copyright © 2003 American Chemical Society)

environmental problems, including the decline of petroleum feedstock and generation of unnecessary byproducts. An example is given here for the production of cyclohexane-carboxylic acid by the hydrogenation of benzoic acid using cluster complex derived nanocatalysts,  $\text{Ru}_5\text{Pt}_1$ ,  $\text{Ru}_{10}\text{Pt}_2$ ,  $\text{Pd}_6\text{Ru}_6$ ,  $\text{Ru}_6\text{Sn}$ , and  $\text{Cu}_4\text{Ru}_{12}$ . Three products could be obtained from the hydrogenation of benzoic acid (Fig. 2.12a), but only the fully hydrogenated product cyclohexane-carboxylic acid is desired because it has been used to produce Caprolactam, which is a precursor to

synthesize Nylon 6 via ring opening polymerization (ROP) in industry. The selectivity results of this catalytic hydrogenation are shown in Fig. 2.12b; the RuPt bimetallic nanocatalyst is the most efficient catalyst in terms of selectivity and conversion compared to other nanocatalysts. Interestingly, when larger metal cluster complexes were used as the catalyst precursor, Ru<sub>10</sub>Pt<sub>2</sub> has the same Ru:Pt ratio as Ru<sub>5</sub>Pt; an increase in reagent conversion was observed. Remarkably, the catalyst generated from Ru<sub>10</sub>Pt<sub>2</sub> shows almost 100% selectivity for the desired product at almost double the TOF (Turnover Frequency) compared to that generated from the Ru<sub>5</sub>Pt cluster.

### 2.3.2 Heavy Main Group Metal Modified Transition Metal Clusters as Supported Catalysts for Hydrogenation

Main group metals, such as group 14 and 15 elements, Ge [108–110], Sn [111–120], Bi [121, 122], Sb, have been shown to be valuable modifiers for transition metal-based catalysts to enhance their catalytic performance and lifetime of the catalysts, especially Pt-based bimetallic catalysts. Bismuth on oxide supports has been shown to catalyze the oxidation of certain hydrocarbons efficiently [121, 122]. Transition metal–bismuth bimetallic catalysts also attracted significant attention since the discovery of bismuth–molybdate catalysts in the 1980s, which catalyzes the important industrial process for the ammoxidation of propylene to acrylonitrile [123]. Studies of the mechanism of this reaction have been suggested that bismuth is responsible for the abstraction of hydrogen from propylene through the Bi–O bond. Heterogeneous nanocatalysts of compositions Re<sub>2</sub>Bi<sub>2</sub>, Re<sub>2</sub>Sb<sub>2</sub>, Re<sub>2</sub>Sb derived from molecular cluster of Re<sub>2</sub>(CO)<sub>8</sub>(μ-BiPh<sub>2</sub>)<sub>2</sub>, Re<sub>2</sub>(CO)<sub>8</sub>(μ-SbPh<sub>2</sub>)<sub>2</sub>, and Re<sub>2</sub>(CO)<sub>8</sub>(μ-SbPh<sub>2</sub>)(μ-H), respectively, have been used in the synthesis of niacin (vitamin B3) for the liquid-phase ammoxidation of 3-picoline to nicotinonitrile (an intermediate to niacin) under mild condition [124]. Later, one step synthesis of niacin by oxidation of 3-picoline using APB (acetylperoxyborate) was achieved by using Ir<sub>3</sub>Bi and Ir<sub>5</sub>Bi<sub>3</sub> nanocatalysts, obtained by thermal activation of the clusters [Ir<sub>3</sub>(CO)<sub>9</sub>(μ<sub>3</sub>-Bi)] and [Ir<sub>5</sub>(CO)<sub>10</sub>(μ<sub>3</sub>-Bi)<sub>2</sub>(μ<sub>4</sub>-Bi)] [125]. The heterometallic complex [Bi<sub>2</sub>Pd<sub>2</sub>(O<sub>2</sub>CCF<sub>3</sub>)<sub>10</sub>(HO<sub>2</sub>CCF<sub>3</sub>)<sub>2</sub>] was used as precursor to prepare carbon-supported PdBi catalyst for the oxidation of D-glucose [126].

Tin has also been shown as valuable modifier to many other transition metal catalysts. Iridium-tin catalysts have been shown to have high selectivity for dehydrogenation of propane to propene [127]. Nickel-tin catalysts have been shown to produce hydrogen catalytically from biomass-derived oxygenated hydrocarbons [128]. Platinum-tin nanoparticles supported on alumina that are used as dehydrogenation and aromatization catalysts have shown to be even more effective than Pt-Re and Pt-Ir bimetallic catalysts in petroleum reforming [19]. The platinum-tin catalysts possess increased reforming selectivity and reduced poisoning by weakening Pt–C bonds that lead to the formation of coke. Many studies have been conducted to try to



understand the role of tin in bimetallic catalysts considering the fact that Pt surface should be poisoned by even small traces of metallic tin [21]. Dautzenberg and Biloen have suggested that tin divides the surface to very small ensembles of platinum atoms (ensemble effect); thus, the hydrogenolysis and isomerization can be suppressed to reduce coke formation [129, 130]. However, Burch and Garla proposed that tin modifies the electronic properties of the small platinum particles (ligand effect), which is attributed to the higher stability and selectivity. Lead has also been used as catalytic modifier in bimetallic transition metal catalysts, but to a lesser extent and not in heterogeneous catalysis system. For instance, a Pd–Pb complex  $[\text{PdPb}(\text{OAc})_4]$  (where OAc is the acetate,  $\text{C}_2\text{H}_3\text{O}_2$  ligand) was used in the benzylic acyloxylation of alkyl aromatics in liquid phase [131].

Among these heavy main group metal modifiers, group 14 elements, germanium and tin draw particular extensive attention for heterogeneous hydrogenation reactions [132]. Rh–Ge bimetallic catalysts supported on alumina prepared by surface redox reaction exhibited exceptional product selectivity of citral hydrogenation to the unsaturated alcohols (nerol and geraniol), which are crucial feedstock for several industries, such as flavor, fragrance, and pharmaceutical industry. On the other hand, the monometallic rhodium catalysts lead to the undesired saturated aldehyde (citronellal) as major product [108]. Tin-containing nanoscale catalysts platinum-tin, rhodium-tin, and ruthenium-tin anchored with mesoporous silica are shown to exhibit remarkable selectivity for the selective hydrogenation (as shown in Fig. 2.13a) of 1,5,9-cyclododecatriene (CDT) to produce cyclododecene (CDE) [133]. By contrast, hydrogenation of CDT by using most simple catalysts readily gives cyclododecane (CDA) as the final product from which all three  $\text{C}=\text{C}$  bonds are hydrogenated. However, CDE is more desired product which is the vital feedstock in many industrial processes. The lone  $\text{C}=\text{C}$  double bond in CDE is easily functionalized and thus can be used to produce a variety of C12 products including precursors to polyesters and nylon-12. Bimetallic organometallic transition metal cluster complexes are used as precursors to prepare the catalysts which are synthesized by deposition of organometallic cluster complexes from solution onto silica supports such as Davison type 911, following by ligand removal by heating in vacuo for 1 h at 473 K. The corresponding parent cluster complexes used for the nanocatalysts of  $\text{PtSn}_2$ ,  $\text{RhSn}_2$ , and  $\text{RuSn}_2$  are  $(\text{COD})\text{Pt}(\text{SnPh}_3)_2$ ,  $(\text{COD} = 1,5\text{-cyclooctadiene})$ ,  $\text{Rh}_3(\text{CO})_6(\text{SnPh}_3)_2(\mu\text{-SnPh})_2$ , and  $\text{Ru}(\text{CO})_4(\text{SnPh}_3)_2$ , respectively. To compare the catalytic performance with the pure PGM (platinum group metals),  $\text{Pt}(\text{COD})_2$ ,  $\text{Rh}_4(\text{CO})_{12}$ , and  $\text{Ru}_3(\text{CO})_{12}$  were used as the precursors to prepare the corresponding monometallic catalysts in the same way as those bimetallic catalysts. The result of the catalytic performance is shown in Fig. 2.13b, which clearly shows in exceptional selective hydrogenation of cluster-derived supported tin-containing bimetallic catalysts. Moreover, Ru–Sn nanocatalysts with different ratios of Ru:Sn from molecular cluster complexes  $[\text{Ru}_4(\mu_4\text{-SnPh})_2(\text{CO})_{12}]$ ,  $[\text{Ru}_4(\mu_4\text{-SnPh})_2(\mu\text{-SnPh}_2)_2(\mu\text{-CO})_2(\text{CO})_8]$ ,  $[\text{Ru}_4(\mu_4\text{-SnPh})_2(\mu\text{-SnPh}_2)_4(\text{CO})_8]$ ,  $[\text{Ru}_6(\mu_6\text{-C})(\text{CO})_{16}(\mu\text{-SnCl}_3)]^-$ , and  $\text{PtRu}_5(\text{CO})_{16}(\mu\text{-SnPh}_2)(\mu_6\text{-C})$  are also evaluated for

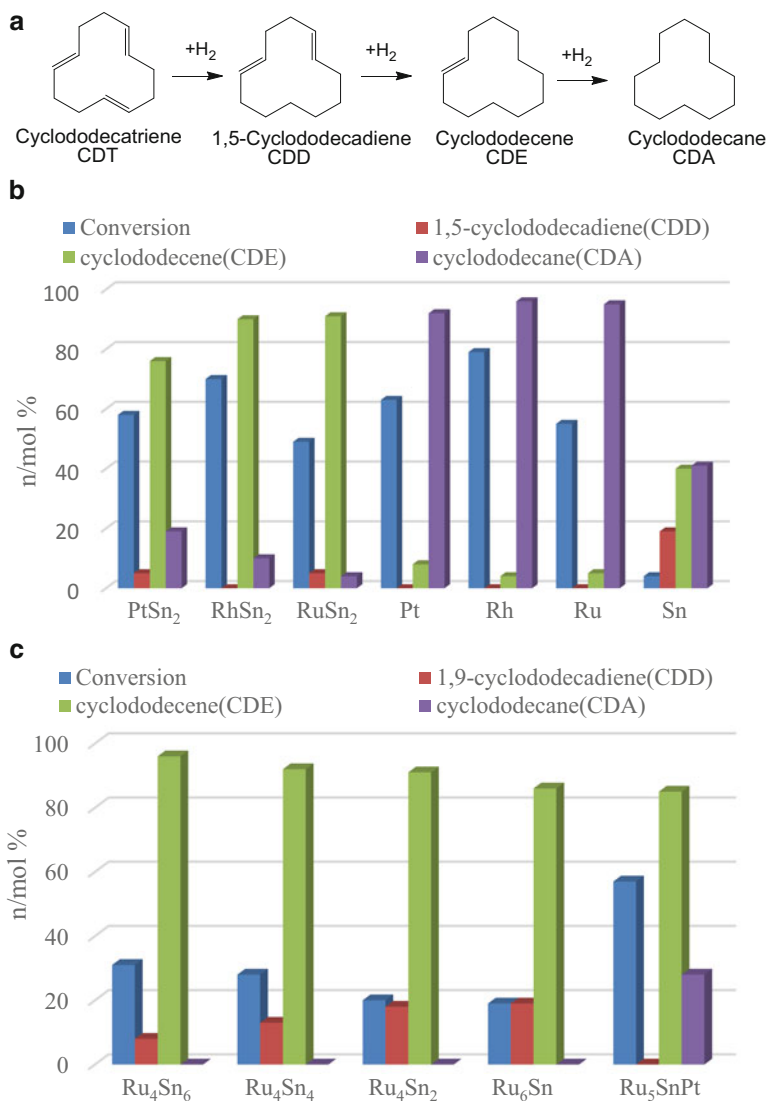


**Fig. 2.13** (a) Stepwise hydrogenation reaction of 1,5,9-cyclododecatriene (CDT). (b) Effect of tin in the selective hydrogenation of CDT using anchored monometallic and bimetallic cluster catalysts. (c) Comparison of catalytic performance of Ru<sub>4</sub>Sn<sub>6</sub>, Ru<sub>4</sub>Sn<sub>4</sub>, Ru<sub>4</sub>Sn<sub>2</sub>, Ru<sub>6</sub>Sn, and Ru<sub>5</sub>SnPt. Reaction conditions: substrate 50 g, catalyst 25 mg (cluster anchored on mesopore 2% metal loading), H<sub>2</sub> pressure 30 bar, T = 373 K, t = 8 h. n/mol% represents the conversion (%) into product

selective hydrogenation of CDT (result see Fig. 2.13c). By incorporation of tin as modifier to platinum group metals, the selectivity and catalytic efficiency are significantly enhanced.

---

## 2.4 Summary

Hydrogen is considered as the most possible alternative energy carrier, and the activation of H–H bond is a very important aspect of chemistry. Hydrogen activation plays a very important role in hydrogenation, hydro-formylation, and hydrogenolysis processes which are key reactions in chemical refining, fuel production, and drug development. Transition metal complexes have been extensively studied as dihydrogen activation catalysts. Considerable amount of efforts have been made during the last century in order to design and synthesis of promising complexes as homogenous or heterogeneous catalysts for hydrogen activation or to serve as biomimetic models to study the hydrogen activation or production mechanisms. In the course of pursuing insights about hydrogen activation, researchers have developed numbers of techniques and methodologies to assist the characterization of reaction intermediates. For example, the development of single crystal X-ray analysis and proton NMR spectroscopy has helped with the determination of complex structures that involve hydrogen molecule or hydrogen atoms. In some rare cases, neutron diffraction is used to precisely locate hydrogen atoms. If iron is involved in the complex, Mössbauer spectroscopy can also be used to determine the oxidation states of the iron centers. It is no doubt that computational chemistry, especially DFT calculations in conjunction with other characterization methods, contributed tremendously to the development of this field.

This chapter summarized some history and recent development in the field of transition metal complexes that are important in hydrogen activation. The hydrogen activation can be classified into two categories, homolytic and heterolytic cleavage. The former normally happens on mononuclear metal complexes, while in most of the cases, dihydrogen molecule will undergo heterolytic cleavage to form a proton and a hydride. Dinuclear transition metal cluster complexes are vital in hydrogen activation not only because they are easy to prepare, but they also play crucial roles in biological systems, namely hydrogenase. Multinuclear transition metal cluster complexes, interestingly, can bind hydrogen molecule reversibly under mild conditions. Numbers of these cluster complexes show very high activity and selectivity for hydrogenation reactions either in solution or deposited on support. In sum, the transition metal complexes in hydrogen activation is a very interesting and important topic which has made considerable progress. With the assistance of current resources and technology, hydrogen activation mechanism will be fully established, which will play an important role in designing new catalysts and will greatly impact the chemical industry and contribute considerably to our daily life.

**Acknowledgement** The technical support from the Departments of Chemistry at Texas A&M University and Washington State University were duly acknowledged.

## References

1. J.N. Armor, Catalysis and the hydrogen economy. *Catal. Lett.* **101**(3–4), 131–135 (2005)
2. J.M. Thomas, R. Raja, B.F.G. Johnson, S. Hermans, M.D. Jones, T. Khimiyak, Bimetallic catalysts and their relevance to the hydrogen economy. *Ind. Eng. Chem. Res.* **42**(8), 1563–1570 (2003)
3. S.S. Bath, L. Vaska, Five-coordinate hydrido-carbonyl complexes of rhodium and iridium and their analogy with  $\text{CoH}(\text{CO})_4$ . *J. Am. Chem. Soc.* **85**(21), 3500–3501 (1963)
4. F. Maseras, A. Lledós, E. Clot, O. Eisenstein, Transition metal polyhydrides: from qualitative ideas to reliable computational studies. *Chem. Rev.* **100**(2), 601–636 (2000)
5. W. Hieber, F. Leutert, Zur Kenntnis des koordinativ gebundenen Kohlenoxyds: Bildung von Eisencarbonylwasserstoff. *Naturwissenschaften* **19**(17), 360–361 (1931)
6. P.J. Craig, The organometallic chemistry of the transition metals. R H Crabtree, John Wiley and Sons (Wiley Interscience), New York, Chichester, Brisbane, Toronto, Singapore, 1988. £36.45. ISBN 0 471853062. *Appl. Organomet. Chem.* **3**(6), 563 (1989)
7. P.J. Brothers, Heterolytic activation of hydrogen by transition metal complexes, in *Prog. Inorg. Chem.* (Wiley, New York, 2007), pp. 1–61
8. M.M.T. Khan, A.E. Martell, 1 – Activation of molecular hydrogen, in *Activation of Small Inorganic Molecules*, ed. by M.M.T.K.E. Martell (Academic, New York, 1974), pp. 1–77
9. G.J. Kubas, R.R. Ryan, B.I. Swanson, P.J. Vergamini, H.J. Wasserman, Characterization of the first examples of isolable molecular hydrogen complexes,  $\text{M}(\text{CO})_3(\text{PR}_3)_2(\text{H}_2)$  ( $\text{M}$  = molybdenum or tungsten;  $\text{R}$  = Cy or isopropyl). Evidence for a side-on bonded dihydrogen ligand. *J. Am. Chem. Soc.* **106**(2), 451–452 (1984)
10. J. Kubas Gregory, Molecular hydrogen complexes: coordination of a sigma. bond to transition metals. *Acc. Chem. Res.* **21**(3), 120–128 (1988)
11. G.J. Kubas, *Metal Dihydrogen and Bond Complexes: Structure Theory and Reactivity* (Kluwer Academic/Plenum Publishers, New York, 2011), p. 472
12. P.G. Jessop, R.H. Morris, Reactions of transition metal dihydrogen complexes. *Coord. Chem. Rev.* **121**, 155–284 (1992)
13. H. Berke, Conceptual approach to the reactivity of dihydrogen. *ChemPhysChem* **11**(9), 1837–1849 (2010)
14. G.J. Kubas, Fundamentals of  $\text{H}_2$  binding and reactivity on transition metals underlying hydrogenase function and  $\text{H}_2$  production and storage. *Chem. Rev.* **107**(10), 4152–4205 (2007)
15. J. Halpern, The catalytic activation of hydrogen in homogeneous, heterogeneous, and biological systems, in *Advances in Catalysis*, ed. by D.D. Eley, P. W. S., B.W. Paul, vol 11 (Academic, New York, 1959), pp. 301–370
16. C. Pettinari, F. Marchetti, D. Martini, Metal complexes as hydrogenation catalysts, in *Comprehensive Coordination Chemistry II*, ed. by J.A.M.J. Meyer (Pergamon, Oxford, 2003), pp. 75–139
17. B.R. James, Hydrogenation reactions catalyzed by transition metal complexes, in *Adv. Organomet. Chem.* ed. by F.G.A. Stone, W. Robert, vol 17 (Academic, New York, 1979), pp. 319–405
18. L.A. Oro, D. Carmona, Rhodium, in *The Handbook of Homogeneous Hydrogenation* (Wiley-VCH Verlag GmbH, Weinheim, 2008), pp. 2–30
19. R.H. Crabtree, Iridium, in *The Handbook of Homogeneous Hydrogenation* (Wiley-VCH Verlag GmbH, Weinheim, 2008), pp. 31–44
20. J.A. Osborn, F.H. Jardine, J.F. Young, G. Wilkinson, The preparation and properties of tris (triphenylphosphine)halogenorhodium(I) and some reactions thereof including catalytic homogeneous hydrogenation of olefins and acetylenes and their derivatives. *J. Chem. Soc. A: Inorg. Phys. Theor.* (0), 1711–1732 (1966)
21. R.R. Schrock, J.A. Osborn, Catalytic hydrogenation using cationic rhodium complexes. 3. The selective hydrogenation of dienes to monoenes. *J. Am. Chem. Soc.* **98**(15), 4450–4455 (1976)

22. R. Crabtree, Iridium compounds in catalysis. *Acc. Chem. Res.* **12**(9), 331–337 (1979)
23. P. Gallezot, Hydrogenation – heterogeneous, in *Encyclopedia of Catalysis* (Wiley, New York, 2002)
24. I. Horiuti, M. Polanyi, Exchange reactions of hydrogen on metallic catalysts. *Trans. Faraday Soc.* **30**, 1164–1172 (1934)
25. E.L. Muetterties, T.N. Rhodin, E. Band, C.F. Brucker, W.R. Pretzer, Clusters and surfaces. *Chem. Rev.* **79**(2), 91–137 (1979)
26. E.L. Muetterties, S.T. Olin, Metal clusters in catalysis VIII. Reduction of triple bonds. *Bull. Soc. Chim. Belg.* **85**(7), 451–470 (1976)
27. M.Y. Darensbourg, E.J. Lyon, J.J. Smee, The bio-organometallic chemistry of active site iron in hydrogenases. *Coord. Chem. Rev.* **206–207**, 533–561 (2000)
28. L. Vaska, J.W. DiLuzio, Activation of hydrogen by a transition metal complex at normal conditions leading to a stable molecular dihydride. *J. Am. Chem. Soc.* **84**(4), 679–680 (1962)
29. C.E. Johnson, R. Eisenberg, Stereoselective oxidative addition of hydrogen to iridium(I) complexes. Kinetic control based on ligand electronic effects. *J. Am. Chem. Soc.* **107**(11), 3148–3160 (1985)
30. G.J. Kubas, R.R. Ryan, D.A. Wroblewski, Molecular hydrogen complexes of the transition metals. 3. Evidence for a new complex,  $\text{Mo}(\text{CO})(\text{dppe})_2(\text{H}_2)$ , and for solution equilibrium between dihydrogen and dihydride forms, M- $\eta^2$ -H<sub>2</sub>-d<sub>blarw</sub>-H-M-H, in  $\text{M}(\text{CO})_3(\text{PR}_3)_2(\text{H}_2)$ . *J. Am. Chem. Soc.* **108**(6), 1339–1341 (1986)
31. M.T. Haward, M.W. George, P. Hamley, M. Poliakoff, Dihydride versus dihydrogen complex; the photochemical reaction of  $(\eta^5\text{-C}_5\text{H}_5)\text{M}(\text{CO})_4$  (M = V, Nb and Ta) with hydrogen in solution at both cryogenic and room temperatures. *J. Chem. Soc. Chem. Commun.* (16), 1101–1103 (1991)
32. D.M. Heinekey, J.K. Law, S.M. Schultz, Kubas complexes revisited: novel dihydride complexes of tungsten. *J. Am. Chem. Soc.* **123**(50), 12728–12729 (2001)
33. G.J. Kubas, R.R. Ryan, C.J. Unkefer, Molecular hydrogen complexes. 5. Electronic control of  $\eta^2\text{-H}_2$  vs. dihydride coordination. Dihydride structure of  $\text{MoH}_2(\text{CO})(\text{R}_2\text{PC}_2\text{H}_4\text{PR}_2)_2$  for R = Et, iso-Bu versus  $\eta^2\text{-H}_2$  for R = Ph. *J. Am. Chem. Soc.* **109**(26), 8113–8115 (1987)
34. G.J. Kubas, C.J. Burns, J. Eckert, S.W. Johnson, A.C. Larson, P.J. Vergamini, C.J. Unkefer, G.R.K. Khalsa, S.A. Jackson, O. Eisenstein, Neutron structure and inelastic-neutron-scattering and theoretical studies of molybdenum complex  $\text{Mo}(\text{CO})(\text{H}_2)[(\text{C}_6\text{D}_5)_2\text{PC}_2\text{H}_4\text{P}(\text{C}_6\text{D}_5)_2]_2\text{-4.5C}_6\text{D}_6$ , a complex with an extremely low barrier to hydrogen rotation. Implications on the reaction coordinate for H-H cleavage to dihydride. *J. Am. Chem. Soc.* **115**(2), 569–581 (1993)
35. R.H. Crabtree, M. Lavin, C-H and H-H bond activation; dissociative vs. nondissociative binding to iridium. *J. Chem. Soc. Chem. Commun.* (12), 794–795 (1985)
36. A.N. Khlobystov, A.J. Blake, N.R. Champness, D.A. Lemenovskii, A.G. Majouga, N.V. Zyk, M. Schröder, Supramolecular design of one-dimensional coordination polymers based on silver(I) complexes of aromatic nitrogen-donor ligands. *Coord. Chem. Rev.* **222**(1), 155–192 (2001)
37. J. Tomàs, A. Lledós, Y. Jean, The Kubas complex revisited. A theoretical study of dihydrogen addition and structure of the dihydride form. *Organometallics* **17**(2), 190–195 (1998)
38. F. Maseras, M. Duran, A. Lledós, J. Bertran, Molecular hydrogen complexes with a hydride ligand. An ab initio study on the iron hydride,  $[\text{Fe}(\text{PR}_3)_4\text{H}(\text{H}_2)]^+$ , system. *J. Am. Chem. Soc.* **113**(8), 2879–2884 (1991)
39. J. Pospech, I. Fleischer, R. Franke, S. Buchholz, M. Beller, Alternative metals for homogeneous catalyzed hydroformylation reactions. *Angew. Chem. Int. Ed.* **52**(10), 2852–2872 (2013)
40. S. Tan, C.T. Williams, An in situ spectroscopic study of prochiral reactant–chiral modifier interactions on palladium catalyst: case of alkenoic acid and cinchonidine in various solvents. *J. Phys. Chem. C* **117**(35), 18043–18052 (2013)
41. S. Tan, J. Monnier, C. Williams, Kinetic study of asymmetric hydrogenation of  $\alpha$ ,  $\beta$ -unsaturated carboxylic acid over cinchona-modified Pd/Al<sub>2</sub>O<sub>3</sub> catalyst. *Top. Catal.* **55**(7–10), 512–517 (2012)

42. R. Noyori, H. Takaya, BINAP: an efficient chiral element for asymmetric catalysis. *Acc. Chem. Res.* **23**(10), 345–350 (1990)
43. T. Hayashi, Chiral monodentate phosphine ligand MOP for transition-metal-catalyzed asymmetric reactions. *Acc. Chem. Res.* **33**(6), 354–362 (2000)
44. M.J. Burk, Modular phospholane ligands in asymmetric catalysis. *Acc. Chem. Res.* **33**(6), 363–372 (2000)
45. W.S. Knowles, Asymmetric hydrogenation. *Acc. Chem. Res.* **16**(3), 106–112 (1983)
46. W.S. Knowles, Application of organometallic catalysis to the commercial production of L-DOPA. *J. Chem. Educ.* **63**(3), 222 (1986)
47. J. Halpern, 2 – Asymmetric catalytic hydrogenation: mechanism and origin of enantioselection, in *Asymmetric Synthesis*, ed. by J.D. Morrison (Academic, San Diego, 1985), pp. 41–69
48. I.D. Gridnev, T. Imamoto, On the mechanism of stereoselection in Rh-catalyzed asymmetric hydrogenation: a general approach for predicting the sense of enantioselectivity. *Acc. Chem. Res.* **37**(9), 633–644 (2004)
49. C.R. Landis, J. Halpern, Asymmetric hydrogenation of methyl (Z)-.alpha.-acetamidocinnamate catalyzed by [1,2-bis(phenyl-o-anisoyl)phosphino]ethane]rhodium(I): kinetics, mechanism and origin of enantioselection. *J. Am. Chem. Soc.* **109**(6), 1746–1754 (1987)
50. R. Noyori, T. Ohkuma, M. Kitamura, H. Takaya, N. Sayo, H. Kumobayashi, S. Akutagawa, Asymmetric hydrogenation of  $\beta$ -keto carboxylic esters. A practical, purely chemical access to  $\beta$ -hydroxy esters in high enantiomeric purity. *J. Am. Chem. Soc.* **109**(19), 5856–5858 (1987)
51. T. Liu, D.L. DuBois, R.M. Bullock, An iron complex with pendent amines as a molecular electrocatalyst for oxidation of hydrogen. *Nat. Chem.* **5**(3), 228–233 (2013)
52. D.M.P. Mingos, Polyhedral skeletal electron pair approach. *Acc. Chem. Res.* **17**(9), 311–319 (1984)
53. A.S. Weller, J.S. McIndoe, Reversible binding of dihydrogen in multimetallic complexes. *Eur. J. Inorg. Chem.* **2007**(28), 4411–4423 (2007)
54. R.W. Broach, J.M. Williams, Interaction of hydrogen and hydrocarbons with transition metals. Neutron diffraction study of di- $\mu$ -hydrido-decacarbonyltriosmium,  $(\mu\text{-H})_2\text{Os}_3(\text{CO})_{10}$ , containing a four-center four-electron hydrogen-osmium ( $\text{H}_2\text{Os}_2$ ) bond. *Inorg. Chem.* **18**(2), 314–319 (1979)
55. R.D. Wilson, R. Bau, The molecular structure of dodecacarbonyltetra- $\mu$ -3-hydrotetrarhenium. Evidence for face-bridging hydrogen atoms. *J. Am. Chem. Soc.* **98**(15), 4687–4689 (1976)
56. R.D. Adams, Y. Kan, Q. Zhang, M.B. Hall, E. Trufan, Bonding and reactivity in the electronically unsaturated hydrogen-bridged dimer  $[\text{Ru}_3(\text{CO})_8(\mu_3\text{-CMe})(\mu\text{-H})_2(\mu_3\text{-H})]_2$ . *Organometallics* **31**(1), 50–53 (2012)
57. M.J. Ingleson, M.F. Mahon, P.R. Raithby, A.S. Weller,  $[(^1\text{Pr}_3\text{P})_6\text{Rh}_6\text{H}_{12}]^{2+}$ : a high-hydride content octahedron that bridges the gap between late and early transition metal clusters. *J. Am. Chem. Soc.* **126**(15), 4784–4785 (2004)
58. S.K. Brayshaw, M.J. Ingleson, J.C. Green, P.R. Raithby, G. Kociok-Köhn, J.S. McIndoe, A.S. Weller, Holding onto lots of hydrogen: a 12-hydride rhodium cluster that reversibly adds two molecules of  $\text{H}_2$ . *Angew. Chem. Int. Ed.* **44**(42), 6875–6878 (2005)
59. R.D. Adams, B. Captain, Hydrogen activation by unsaturated mixed-metal cluster complexes: new directions. *Angew. Chem. Int. Ed.* **47**(2), 252–257 (2008)
60. R.D. Adams, B. Captain, L. Zhu, Facile activation of hydrogen by an unsaturated platinum–osmium cluster complex. *J. Am. Chem. Soc.* **129**(9), 2454–2455 (2007)
61. R.D. Adams, B. Captain, A highly unsaturated platinum–rhenium cluster complex that adds an unusually large amount of hydrogen. *Angew. Chem. Int. Ed.* **44**(17), 2531–2533 (2005)
62. R.D. Adams, B. Captain, C. Beddie, M.B. Hall, Photoreversible multiple additions of hydrogen to a highly unsaturated platinum–rhenium cluster complex. *J. Am. Chem. Soc.* **129**(4), 986–1000 (2007)

63. R.D. Adams, B. Captain, Unusual structures and reactivity of mixed metal cluster complexes containing the palladium/platinum Tri-*t*-butylphosphine grouping. *Acc. Chem. Res.* **42**(3), 409–418 (2009)
64. J.F. Harrod, A.J. Chalk, Homogeneous catalysis. III. Isomerization of deuterio olefins by group VIII metal complexes. *J. Am. Chem. Soc.* **88**(15), 3491–3497 (1966)
65. R.D. Adams, T.S. Barnard, Z. Li, W. Wu, J. Yamamoto, Catalytic hydrogenation of diphenylacetylene by a layer-segregated platinum-ruthenium cluster complex. *J. Am. Chem. Soc.* **116**(20), 9103–9113 (1994)
66. A. Volbeda, L. Martin, C. Cavazza, M. Matho, B. Faber, W. Roseboom, S.J. Albracht, E. Garcin, M. Rousset, J. Fontecilla-Camps, Structural differences between the ready and unready oxidized states of [NiFe] hydrogenases. *JBIC* **10**(3), 239–249 (2005)
67. E. Garcin, X. Vernede, E.C. Hatchikian, A. Volbeda, M. Frey, J.C. Fontecilla-Camps, The crystal structure of a reduced [NiFeSe] hydrogenase provides an image of the activated catalytic center. *Structure* **7**(5), 557–566 (1999)
68. A. Volbeda, E. Garcin, C. Piras, A.L. de Lacey, V.M. Fernandez, E.C. Hatchikian, M. Frey, J.C. Fontecilla-Camps, Structure of the [NiFe] hydrogenase active site: evidence for biologically uncommon Fe ligands. *J. Am. Chem. Soc.* **118**(51), 12989–12996 (1996)
69. H. Ogata, Y. Mizoguchi, N. Mizuno, K. Miki, S.-I. Adachi, N. Yasuoka, T. Yagi, O. Yamauchi, S. Hirota, Y. Higuchi, Structural studies of the carbon monoxide complex of [NiFe]hydrogenase from *Desulfovibrio vulgaris* Miyazaki F: suggestion for the initial activation site for dihydrogen. *J. Am. Chem. Soc.* **124**(39), 11628–11635 (2002)
70. Y. Montet, P. Amara, A. Volbeda, X. Vernede, E.C. Hatchikian, M.J. Field, M. Frey, J.C. Fontecilla-Camps, Gas access to the active site of Ni-Fe hydrogenases probed by X-ray crystallography and molecular dynamics. *Nat. Struct. Mol. Biol.* **4**(7), 523–526 (1997)
71. P.E.M. Siegbahn, J.W. Tye, M.B. Hall, Computational studies of [NiFe] and [FeFe] hydrogenases. *Chem. Rev.* **107**(10), 4414–4435 (2007)
72. M. Bruschi, M. Tiberti, A. Guerra, L. De Gioia, Disclosure of key stereoelectronic factors for efficient H<sub>2</sub> binding and cleavage in the active site of [NiFe]-hydrogenases. *J. Am. Chem. Soc.* **136**(5), 1803–1814 (2014)
73. W. Lubitz, H. Ogata, O. Rüdiger, E. Reijerse, Hydrogenases. *Chem. Rev.* **114**(8), 4081–4148 (2014)
74. M. Brecht, M. van Gastel, T. Buhrke, B. Friedrich, W. Lubitz, Direct detection of a hydrogen ligand in the [NiFe] center of the regulatory H<sub>2</sub>-sensing hydrogenase from *Ralstonia eutropha* in its reduced state by HYSCORE and ENDOR spectroscopy. *J. Am. Chem. Soc.* **125**(43), 13075–13083 (2003)
75. J.P. Whitehead, R.J. Gurbiel, C. Bagyinka, B.M. Hoffman, M.J. Maroney, The hydrogen binding site in hydrogenase: 35-GHz ENDOR and XAS studies of the nickel-C (reduced and active form) and the Ni-L photoproduct. *J. Am. Chem. Soc.* **115**(13), 5629–5635 (1993)
76. C. Tard, C.J. Pickett, Structural and functional analogues of the active sites of the [Fe]-, [NiFe]-, and [FeFe]-hydrogenases. *Chem. Rev.* **109**(6), 2245–2274 (2009)
77. Y. Ohki, K. Tatsumi, Thiolate-bridged iron–nickel models for the active site of [NiFe] hydrogenase. *Eur. J. Inorg. Chem.* **2011**(7), 973–985 (2011)
78. F. Gloaguen, T.B. Rauchfuss, Small molecule mimics of hydrogenases: hydrides and redox. *Chem. Soc. Rev.* **38**(1), 100–108 (2009)
79. J.M. Camara, T.B. Rauchfuss, Combining acid–base, redox and substrate binding functionalities to give a complete model for the [FeFe]-hydrogenase. *Nat. Chem.* **4**(1), 26–30 (2012)
80. M. Ichikawa, Metal cluster compounds as molecular precursors for tailored metal catalysts, in *Advances in Catalysis*, ed. by D.D. Eley, H. P., B.W. Paul, vol 38 (Academic, New York, 1992), pp. 283–400
81. D.W. Goodman, J.E. Houston, Catalysis: new perspectives from surface science. *Science* **236** (4800), 403–409 (1987)
82. J. Xiao, R.J. Puddephatt, Pt-Re clusters and bimetallic catalysts. *Coord. Chem. Rev.* **143**, 457–500 (1995)

83. M.J. Dees, V. Ponc, On the influence of sulfur on the platinum/iridium bimetallic catalysts in n-hexane/hydrogen reactions. *J. Catal.* **115**(2), 347–355 (1989)
84. R.W. Rice, K. Lu, Comparison of platinum and platinum-iridium catalysts for heptane reforming at different pressures. *J. Catal.* **77**(1), 104–117 (1982)
85. J.C. Rasser, W.H. Beindorff, J.J.F. Scholten, Characterization and performance of platinum-iridium reforming catalysts. *J. Catal.* **59**(2), 211–222 (1979)
86. J.H. Sinfelt, Bifunctional catalysis, in *Advances in Chemical Engineering*, ed. by T.B. Drew, J. W. H. T. V., R.C. Giles, vol 5 (Academic, New York, 1964), pp. 37–74
87. J. Schwank, Bimetallic catalysts: discoveries, concepts, and applications. By John H. Sinfelt, John Wiley & Sons, 1983. XI+164 pp. *AIChE J.* **31**(8), 1405 (1985)
88. J.H. Sinfelt, G.H. Via, Dispersion and structure of platinum-iridium catalysts. *J. Catal.* **56**(1), 1–11 (1979)
89. B.D. Chandler, A.B. Schabel, C.F. Blanford, L.H. Pignolet, Preparation and characterization of supported bimetallic Pt–Au particle catalysts from molecular cluster and chloride salt precursors. *J. Catal.* **187**(2), 367–384 (1999)
90. B.D. Chandler, A.B. Schabel, L.H. Pignolet, Preparation and characterization of supported bimetallic Pt–Au and Pt–Cu catalysts from bimetallic molecular precursors. *J. Catal.* **193**(2), 186–198 (2000)
91. F. Schüth, K. Unger, Precipitation and coprecipitation, in *Preparation of Solid Catalysts* (Wiley-VCH Verlag GmbH, Weinheim, 2008), pp. 60–84
92. S. Tan, X. Sun, C.T. Williams, In situ ATR-IR study of prochiral 2-methyl-2-pentenoic acid adsorption on Al<sub>2</sub>O<sub>3</sub> and Pd/Al<sub>2</sub>O<sub>3</sub>. *PCCP* **13**(43), 19573–19579 (2011)
93. G. Chen, S. Tan, W.J. Koros, C.W. Jones, Metal organic frameworks for selective adsorption of t-Butyl mercaptan from natural gas. *Energy Fuel* **29**(5), 3312–3321 (2015)
94. Chapter 7: Preparation and characterization of metal and alloy catalysts, in *Stud. Surf. Sci. Catal.*, vol. 95, ed. by P. Vladimir, C. B. Geoffrey (Elsevier, 1995), pp. 299–391
95. L. Mond, C. Langer, F. Quincke, L.-Action of carbon monoxide on nickel. *J. Chem. Soc. Trans.* **57**, 749–753 (1890)
96. A.K. Smith, J.M. Basset, Transition metal cluster complexes as catalysts. A review. *J. Mol. Catal.* **2**(4), 229–241 (1977)
97. J.M. Thomas, B.F.G. Johnson, R. Raja, G. Sankar, P.A. Midgley, High-performance nano-catalysts for single-step hydrogenations. *Acc. Chem. Res.* **36**(1), 20–30 (2003)
98. O.S. Alexeev, B.C. Gates, Supported bimetallic cluster catalysts. *Ind. Eng. Chem. Res.* **42**(8), 1571–1587 (2003)
99. E.G. Mednikov, S.A. Ivanov, I.V. Slovokhotova, L.F. Dahl, Nanosized [Pd<sub>52</sub>(CO)<sub>36</sub>(PET<sub>3</sub>)<sub>14</sub>] and [Pd<sub>66</sub>(CO)<sub>45</sub>(PET<sub>3</sub>)<sub>16</sub>] clusters based on a hypothetical Pd<sub>38</sub> vertex-truncated  $\nu$ 3 octahedron. *Angew. Chem. Int. Ed.* **44**(42), 6848–6854 (2005)
100. N.T. Tran, D.R. Powell, L.F. Dahl, Nanosized Pd<sub>145</sub>(CO)<sub>x</sub>(PET<sub>3</sub>)<sub>30</sub> containing a capped three-shell 145-atom metal-core geometry of pseudo icosahedral symmetry. *Angew. Chem. Int. Ed.* **39**(22), 4121–4125 (2000)
101. S. Zacchini, Using metal carbonyl clusters to develop a molecular approach towards metal nanoparticles. *Eur. J. Inorg. Chem.* **2011**(27), 4125–4145 (2011)
102. R.D. Adams, J.E. Babin, M. Tasi, J.G. Wang, Catalyst design. The activation of a trinuclear metal cluster complex by metal atom substitution. *Organometallics* **7**(3), 755–764 (1988)
103. M. Castiglioni, R. Giordano, E. Sappa, Phosphine-substituted and phosphido-bridged metal clusters in homogeneous catalysis. *J. Organomet. Chem.* **342**(1), 111–127 (1988)
104. M. Castiglioni, R. Giordano, E. Sappa, Homogeneous catalytic hydrogenation and isomerization of linear and cyclic monoenes and dienes in the presence of the heterometallic cluster ( $\eta^5$ -C<sub>5</sub>H<sub>5</sub>)NiRu<sub>3</sub>( $\mu$ -H)<sub>3</sub>(CO)<sub>9</sub>. *J. Organomet. Chem.* **319**(2), 167–181 (1987)
105. B.D. Dombek, Synergistic behavior of homogeneous ruthenium-rhodium catalysts for hydrogenation of carbon monoxide. *Organometallics* **4**(10), 1707–1712 (1985)
106. P. Buchwalter, J. Rosé, P. Braunstein, Multimetallic catalysis based on heterometallic complexes and clusters. *Chem. Rev.* **115**(1), 28–126 (2015)



107. R. Raja, S. Hermans, D. Shephard, B.F.G. Johnson, R. Raja, G. Sankar, S. Bromley, J. Meurig Thomas, Preparation and characterisation of a highly active bimetallic (Pd-Ru) nanoparticle heterogeneous catalyst[dagger]. *Chem. Commun.* (16), 1571–1572 (1999)
108. T. Ekou, A. Vicente, G. Lafaye, C. Especel, P. Marecot, Bimetallic Rh-Ge and Pt-Ge catalysts supported on TiO<sub>2</sub> for citral hydrogenation: II. Catalytic properties. *Appl. Catal. A Gen.* **314**(1), 73–80 (2006)
109. G. Lafaye, C. Micheaud-Especel, C. Montassier, P. Marecot, Characterization of bimetallic rhodium-germanium catalysts prepared by surface redox reaction. *Appl. Catal. A Gen.* **230**(1–2), 19–30 (2002)
110. G. Jacobs, L. Williams, U. Graham, G.A. Thomas, D.E. Sparks, B.H. Davis, Low temperature water–gas shift: in situ DRIFTS-reaction study of ceria surface area on the evolution of formates on Pt/CeO<sub>2</sub> fuel processing catalysts for fuel cell applications. *Appl. Catal. A Gen.* **252**(1), 107–118 (2003)
111. R. Burch, Platinum-tin reforming catalysts: I. The oxidation state of tin and the interaction between platinum and tin. *J. Catal.* **71**(2), 348–359 (1981)
112. R. Burch, L.C. Garla, Platinum-tin reforming catalysts. *J. Catal.* **71**(2), 360–372 (1981)
113. T. Fujikawa, F.H. Ribeiro, G.A. Somorjai, The effect of Sn on the reactions of n-Hexane and cyclohexane over polycrystalline Pt foils. *J. Catal.* **178**(1), 58–65 (1998)
114. Y.-K. Park, F.H. Ribeiro, G.A. Somorjai, The effect of potassium and tin on the hydrogenation of ethylene and dehydrogenation of cyclohexane over Pt(111). *J. Catal.* **178**(1), 66–75 (1998)
115. R.D. Cortright, J.A. Dumesic, Microcalorimetric, spectroscopic, and kinetic studies of silica supported Pt and Pt/Sn catalysts for isobutane dehydrogenation. *J. Catal.* **148**(2), 771–778 (1994)
116. F. Epron, C. Carnevillier, P. Marécot, Catalytic properties in n-heptane reforming of Pt–Sn and Pt–Ir–Sn/Al<sub>2</sub>O<sub>3</sub> catalysts prepared by surface redox reaction. *Appl. Catal. A Gen.* **295**(2), 157–169 (2005)
117. G.W. Huber, J.W. Shabaker, J.A. Dumesic, Raney Ni-Sn catalyst for H<sub>2</sub> production from biomass-derived hydrocarbons. *Science* **300**(5628), 2075–2077 (2003)
118. R.D. Cortright, J.M. Hill, J.A. Dumesic, Selective dehydrogenation of isobutane over supported Pt/Sn catalysts. *Catal. Today* **55**(3), 213–223 (2000)
119. S. Hermans, R. Raja, J.M. Thomas, B.F.G. Johnson, G. Sankar, D. Gleeson, Solvent-free, low-temperature, selective hydrogenation of polyenes using a bimetallic nanoparticle Ru–Sn catalyst. *Angew. Chem. Int. Ed.* **40**(7), 1211–1215 (2001)
120. B.F.G. Johnson, S.A. Raynor, D.B. Brown, D.S. Shephard, T. Mashmeyer, J.M. Thomas, S. Hermans, R. Raja, G. Sankar, New catalysts for clean technology. *J. Mol. Catal. A Chem.* **182–183**, 89–97 (2002)
121. D. Dumitriu, R. Bârjega, L. Frunza, D. Macovei, T. Hu, Y. Xie, V.I. Pârvulescu, S. Kaliaguine, BiOx clusters occluded in a ZSM-5 matrix: preparation, characterization, and catalytic behavior in liquid-phase oxidation of hydrocarbons. *J. Catal.* **219**(2), 337–351 (2003)
122. G. Qian, D. Ji, G. Lu, R. Zhao, Y. Qi, J. Suo, Bismuth-containing MCM-41: synthesis, characterization, and catalytic behavior in liquid-phase oxidation of cyclohexane. *J. Catal.* **232**(2), 378–385 (2005)
123. R.K. Grasselli, Selective oxidation and ammoxidation of olefins by heterogeneous catalysis. *J. Chem. Educ.* **63**(3), 216 (1986)
124. R. Raja, R.D. Adams, D.A. Blom, W.C. Pearl, E. Gianotti, J.M. Thomas, New catalytic liquid-phase ammoxidation approach to the preparation of niacin (vitamin B<sub>3</sub>). *Langmuir* **25**(13), 7200–7204 (2009)
125. R.D. Adams, M. Chen, G. Elpitiya, M.E. Potter, R. Raja, Iridium–bismuth cluster complexes yield bimetallic nano-catalysts for the direct oxidation of 3-picoline to niacin. *ACS Catal.* **3**(12), 3106–3110 (2013)
126. B. Li, H. Zhang, L. Huynh, C. Diverchy, S. Hermans, M. Devillers, E.V. Dikarev, Bismuth–palladium heterometallic carboxylate as a single-source precursor for the carbon-supported Pd–Bi/C catalysts. *Inorg. Chem.* **48**(13), 6152–6158 (2009)

127. M. Guidotti, V.D. Santo, A. Gallo, E. Gianotti, G. Peli, R. Psaro, L. Sordelli, Catalytic dehydrogenation of propane over cluster-derived Ir–Sn/SiO<sub>2</sub> catalysts. *Catal. Lett.* **112**(1–2), 89–95 (2006)
128. J.W. Shabaker, D.A. Simonetti, R.D. Cortright, J.A. Dumesic, Sn-modified Ni catalysts for aqueous-phase reforming: characterization and deactivation studies. *J. Catal.* **231**(1), 67–76 (2005)
129. F.M. Dautzenberg, J.N. Helle, P. Biloen, W.M.H. Sachtler, Conversion of n-hexane over monofunctional supported and unsupported PtSn catalysts. *J. Catal.* **63**(1), 119–128 (1980)
130. P. Biloen, J.N. Helle, H. Verbeek, F.M. Dautzenberg, W.M.H. Sachtler, The role of rhenium and sulfur in platinum-based hydrocarbon-conversion catalysts. *J. Catal.* **63**(1), 112–118 (1980)
131. A.B. Goel, P.E. Throckmorton, R.A. Grimm, Homogeneous palladium catalyzed oxidations: a novel, highly effective bimetallic palladium lead acetate complex useful in benzylic acyloxylation of alkyl aromatics. *Inorg. Chim. Acta* **117**(1), L15–L17 (1986)
132. M.S. Holt, W.L. Wilson, J.H. Nelson, Transition metal-tin chemistry. *Chem. Rev.* **89**(1), 11–49 (1989)
133. R.D. Adams, D.A. Blom, B. Captain, R. Raja, J.M. Thomas, E. Trufan, Toward less dependence on platinum group metal catalysts: the merits of utilizing tin. *Langmuir* **24**(17), 9223–9226 (2008)